

ISSN: 2738-9928 (Online)
2738-9812 (Print)

NEPAL JOURNAL OF MATHEMATICAL SCIENCES (NJMS)



Published by

SCHOOL OF MATHEMATICAL SCIENCES

Tribhuvan University, Kirtipur
Kathmandu, Nepal

Volume 5, Number 1

February 2024

NEPAL JOURNAL OF MATHEMATICAL SCIENCES (NJMS)

ISSN: 2738-9928 (Online), 2738-9812 (Print)

Volume-5, Number -1 (February 2024)

Editorial Team

Advisors

Prof. Dr. Shankar Prasad Khanal, Dean, Institute of Science and Technology, Tribhuvan University, Nepal
Assoc. Prof. Nawaraj Paudel, Director, School of Mathematical Sciences, Tribhuvan University, Nepal

Editorial Board

Prof. Dr. Narayan Prasad Pahari (Editor-in-Chief)

Central Department of Mathematics, Tribhuvan University, Kirtipur, Kathmandu, Nepal

Prof. Dr. Subarna Shakya (Member)

Institute of Engineering, Tribhuvan University, Pulchowk, Lalitpur, Nepal

Prof. Dr. Srijan Lal Shrestha (Member)

Central Department of Statistics, Tribhuvan University, Kirtipur, Kathmandu, Nepal

Prof. Dr. Gyan Bahadur Thapa (Member)

Institute of Engineering, Tribhuvan University, Pulchowk, Lalitpur, Nepal

Editors

Prof. Dr. Bal Krishna Bal, Department of Computer Engineering, Kathmandu University, Nepal

Prof. Dr. Binod Chandra Tripathy, Department of Mathematics Tripura University, India

Prof. Dr. Chet Raj Bhatta, Central Department of Mathematics, Tribhuvan University, Nepal

Prof. Dr. Danda Bir Rawat, Department of Computer Science, Howard University, Washington, DC, USA

Prof. Dr. Dil Bahadur Gurung, School of Natural Sciences, Kathmandu University

Prof. Dr. Dinesh Panthi, Department of Mathematics, Nepal Sanskrit University, Nepal

Prof. Dr. Dipak Kumar Jana, Applied Science, Haldia Institute of Technology, W.B., India

Prof. Dr. Jyotsna Kumar Mandal, Department of Computer Sciences, Kalyani University, West Bengal, India

Prof. Dr. Narayan Adhikari, Central Department of Physics, Tribhuvan University, Nepal

Prof. Dr. Ram Prasad Ghimire, School of Natural Sciences, Kathmandu University

Prof. Dr. Vijay Kumar, Department of Statistics, DDU Gorakhpur University, India

Prof. Dr. Vikash Kumar KC, Department of Statistics, Prithwi Narayan Campus, Tribhuvan University, Nepal

Prof. Dr. Vikash Raj Satyal, Department of Statistics, Amrit Campus, Tribhuvan University, Nepal

Dr. Badri Adhikari, Department of Computer Science, University of Missouri-St. Louis, USA

Dr. Bishnu Hari Subedi, Central Department of Mathematics, Tribhuvan University, Nepal

Dr. Chakra Bahadur Khadka, School of Mathematical Sciences, Tribhuvan University, Nepal

Dr. Debendra Banjade, Department of Mathematics, Coastal Carolina University, USA

Dr. Durga Jang KC, Central Department of Mathematics, Tribhuvan University, Nepal

Dr. Ganesh B. Malla, Department of Statistics, University of Cincinnati – Clermont, USA

Dr. Ghanshyam Bhatt, Department of Mathematics, Tennessee State University, USA

Dr. Ishwari Jang Kunwar, Department of Mathematics & Computer Science, Fort Valley State University, USA

Dr. Milan Bimali, Department of Biostatistics, University of Arkansas for Medical Sciences, USA

Dr. Parameshwari Kattel, Dept. of Mathematics, Trichandra Multiple Campus, Tribhuvan University, Nepal

Dr. Rama Shanker, Department of Statistics, Assam University, Silchar, India

Dr. Sahadeb Upretee, Department of Actuarial Science, Central Washington University, USA

Dr. Shree Ram Khadka, Central Department of Mathematics, Tribhuvan University, Nepal

Managing Coordinator

Mr. Keshab Raj Phulara, School of Mathematical Sciences, Tribhuvan University, Nepal

NEPAL JOURNAL OF MATHEMATICAL SCIENCES (NJMS)
Volume-5, Number-1
(February, 2024)

©School of Mathematical Sciences, Tribhuvan University

The views and interpretations in this journal are those of the author(s) and they are not attributable to the School of Mathematical Sciences, Tribhuvan University.

The Nepal Journal of Mathematical Sciences (NJMS) is now available on NepJOL at <https://www.nepjol.info/index.php/njmathsci/index>

MAILING ADDRESS

Nepal Journal of Mathematical Sciences
School of Mathematical Sciences
Tribhuvan University, Kirtipur
Kathmandu, Nepal
Website: www.sms.tu.edu.np
Email: njmseditor@gmail.com

Editorial

We are pleased to present the first issue of Volume 5 for the year 2024 of *Nepal Journal of Mathematical Sciences (NJMS)*. This issue contains five original research articles spanning various fields of mathematics and mathematical sciences. We extend our sincere gratitude to all the authors for contributing their research to this issue. Our heartfelt thanks also go to the reviewers and editors for their invaluable support and guidance, which have been instrumental in bringing this publication on time. We would like to request research scholars, professors, and scientists to consider submitting their original research articles for future issues of NJMS.

February 28, 2025

Editor-in-Chief

CONTENTS

SN	Article Titles and Authors	Page No.
1.	<p>An Integral Involving Generalized Hypergeometric Function</p> <p>□ <i>Ganesh Bahadur Basnet, Narayan Prasad Pahari, Resham Prasad Paudel, Madhav Prasad.Poudel & Mukesh Sharma</i></p> <p>DOI: https://doi.org/10.3126/njmathsci.v5i1.76446</p>	1-6
2.	<p>Study of Common Fixed Point Theorems for Interpolative Contraction in Metric Space</p> <p>□ <i>Surendra Kumar Tiwari & Jayant Prakash Ganvir</i></p> <p>DOI: https://doi.org/10.3126/njmathsci.v5i1.76442</p>	7-14
3.	<p>Security of E-health Image in Cloud Environment Using Hybridization of DNA Cryptography: Systematic Literature Review</p> <p>□ <i>Madhav Dhakal & Subarna Shakya</i></p> <p>DOI: https://doi.org/10.3126/njmathsci.v5i1.76443</p>	15-28
4.	<p>A Short Note in Quantum Continuity Equation</p> <p>□ <i>Bishnu Hari Subedi & Tara Bahadur Rana</i></p> <p>DOI: https://doi.org/10.3126/njmathsci.v5i1.76448</p>	29-34
5.	<p>Mathematical Approach for Estimating the Effective Reproductive Number for COVID-19 in Nepal with Data-Driven SIR Model</p> <p>□ <i>Shiva Hari Subedi & Gyan Bahadur Thapa</i></p> <p>DOI: https://doi.org/10.3126/njmathsci.v5i1.76447</p>	35-44



An Integral Involving Generalized Hypergeometric Function

Ganesh Bahadur Basnet^{1,2}, Narayan Prasad Pahari^{2*}, Resham Prasad Paudel^{1,2},

Madhav Prasad Poudel³ & Mukesh Sharma⁴

¹Department of Mathematics, Tri-Chandra Multiple Campus, Tribhuvan University, Kathmandu, Nepal

²Central Department of Mathematics, Tribhuvan University, Kirtipur, Kathmandu, Nepal

³School of Engineering, Pokhara University, Pokhara, Kaski, Nepal,

⁴ Department of Mathematics, M. L. B. Government College, Nokha, Rajasthan, India.

Corresponding Author : *nppahari@gmail.com

Abstract: In this article, we have evaluated an integral involving a generalized hypergeometric function.

This is achieved by employing a summation formula for the series ${}_4F_3$ obtained earlier by Choi and Rathie [3]. A few special cases have also been given. The result provided in this note is simple, interesting, easily established, and may be useful.

2020 Mathematical subject classification: Primary: 05A15, 33C05, Secondary: 33C15, 33C20

Keywords: Generalized hypergeometric function, Finite integral, Watson theorem, Pochhammer symbol.

1. Introduction

The generalized hypergeometric function, denoted by ${}_pF_q(z)$, characterized by p numerator parameters and q denominators parameters, is defined by [7, 8]

$${}_pF_q \left[\begin{matrix} a_1, a_2, \dots, a_p \\ b_1, b_2, \dots, b_p \end{matrix} ; z \right] = \sum_{n=0}^{\infty} \frac{(a_1)_n (a_2)_n \dots (a_p)_n}{(b_1)_n (b_2)_n \dots (b_p)_n} \frac{z^n}{n!} \quad (1)$$

where $(c)_n$ represent the Pochhammer symbol, which is defined as follows

$$(c)_n = \begin{cases} c(c+1) \dots (c+n-1); & n \in \mathbb{N}, \\ 1 & ; n = 0. \end{cases}$$

Express in terms of gamma function, we obtain

$$(c)_n = \frac{\Gamma(c+n)}{\Gamma(c)}.$$

Here, p and q are non-negative integers and the parameters a_j ($1 \leq j \leq p$) and b_j ($1 \leq j \leq q$) can take arbitrary complex values with zero or negative integer values of b_j excluded [7]. The generalized hypergeometric function ${}_pF_q(z)$ converges for all

$$z < \infty \ (p \leq q), z < 1 \ (p = q + 1) \text{ and } |z| = 1 \ (p = q + 1 \text{ and } \text{Res}(s) > 0,$$

where s is the parametric excess defined by

$$s = \sum_{j=1}^q b_j - \sum_{j=1}^p a_j$$

The generalized hypergeometric function plays a significant role across diverse disciplines due to its broad applicability. Its uses span fields such as mathematics, theoretical physics, engineering, and statistical sciences. For further information on this function, we refer the readers to the references [1,8].

Additionally, in the study of generalized hypergeometric functions, classical summation theorems hold significant importance. These results include Gauss’s summation theorem and Gauss’s second theorem. Additionally, they encompass Bailey’s and Kummer’s theorems for the series ${}_2F_1$. Furthermore, Watson’s, Dixon’s, Whipple’s, and Saalschütz’s theorems apply to the series ${}_3F_2$, among others. In this paper, we specifically highlight the classical Watson’s theorem [1], stated as follows:

$$\begin{aligned}
 {}_3F_2 \left[\begin{matrix} a, b, c \\ \frac{a+b+1}{2}, 2c \end{matrix} ; 1 \right] &= \frac{\Gamma\left(\frac{1}{2}\right)\Gamma\left(c+\frac{1}{2}\right)\Gamma\left(\frac{a}{2}+\frac{b}{2}+\frac{1}{2}\right)\Gamma\left(c-\frac{a}{2}-\frac{b}{2}+\frac{1}{2}\right)}{\Gamma\left(\frac{a}{2}+\frac{1}{2}\right)\Gamma\left(\frac{b}{2}+\frac{1}{2}\right)\Gamma\left(c-\frac{a}{2}+\frac{1}{2}\right)\Gamma\left(c-\frac{b}{2}+\frac{1}{2}\right)} \\
 &= s \text{ (say)} \tag{2}
 \end{aligned}$$

Provided $\text{Re}(2c - a - b) > -1$.

In 1992, Lavoie, et al. [5] classical Watson’s theorem (2), then we obtain the explicit expression of

$${}_3F_2 \left[\begin{matrix} a, b, c \\ \frac{a+b+i+1}{2}, 2c+j \end{matrix} ; 1 \right] \tag{3}$$

for $i, j = 0 \pm 1, \pm 2$.

Clearly for $i = j = 0$, the expression (3) reduces to the Watson’s theorem (2). In the same paper, they have examined numerous fascinating special cases and limiting cases of their main results. In 2010, Kim, et al. [4] established the two interesting extensions of the classical Watson’s summation theorem (2). In 2016, Choi and Rathie [3] established thirteen results including the two results obtained earlier by Kim, et al. [5] with the help of the contiguous results obtained earlier by Lavoie, et al. [5].

Here, we shall mention one result out of the thirteen results which will be essential for our current study.

$${}_4F_3 \left[\begin{matrix} a, b, c, d+1 \\ \frac{a+b+1}{2}, 2c+1, d \end{matrix} ; 1 \right] = \frac{\Gamma\left(\frac{1}{2}\right)\Gamma\left(c+\frac{1}{2}\right)\Gamma\left(\frac{a}{2}+\frac{b}{2}+\frac{1}{2}\right)\Gamma\left(c-\frac{a}{2}-\frac{b}{2}+\frac{1}{2}\right)}{\Gamma\left(\frac{a}{2}+\frac{1}{2}\right)\Gamma\left(\frac{b}{2}+\frac{1}{2}\right)\Gamma\left(c-\frac{a}{2}+\frac{1}{2}\right)\Gamma\left(c-\frac{b}{2}+\frac{1}{2}\right)}$$

$$\begin{aligned}
 & + \left(\frac{2c}{d} - 1\right) \frac{\Gamma\left(\frac{1}{2}\right)\Gamma\left(c + \frac{1}{2}\right)\Gamma\left(\frac{a}{2} + \frac{b}{2} + \frac{1}{2}\right)\Gamma\left(c - \frac{a}{2} - \frac{b}{2} + \frac{1}{2}\right)}{\Gamma\left(\frac{a}{2}\right)\Gamma\left(\frac{b}{2}\right)\Gamma\left(c - \frac{a}{2} + 1\right)\Gamma\left(c - \frac{b}{2} + 1\right)} \\
 & = s_1 \text{ (let)} \tag{4}
 \end{aligned}$$

provided $d \notin \mathbb{Z}_0^-$ and $Re(2c - a - b) > -1$.

It is interesting to mention here that if we take $d = 2c$ in (4), we at once get the classical Watson’s theorem (2). Thus, the result (4) is regarded as an extension of the classical Watson’s summation theorem (2).

In 2024, Basnet, et al.[2] established a result on an integral involving product of two generalized hypergeometric functions. In this research, we have evaluated an interesting integral involving generalized hypergeometric function. This is achieved by employing the summation formula (4) due to the Choi and Rathie in the following integral due to the MacRobert [6]

$$\int_0^{\frac{\pi}{2}} e^{i(\alpha+\beta)\theta} (\sin \theta)^{\alpha-1} (\cos \theta)^{\beta-1} d\theta = e^{i\frac{\pi}{2}(\alpha)} \frac{\Gamma(\alpha)\Gamma(\beta)}{\Gamma(\alpha + \beta)} \tag{5}$$

Provided $R(\alpha) > 0$ and $R(\beta) > 0$.

Several special cases have also been presented. The result in this paper is straightforward, intriguing, easy to derive, and potentially useful.

2. Main Result

In this section, we shall evaluate the following integral asserted in the theorem.

Theorem 2.1

$$\int_0^{\frac{\pi}{2}} e^{i(2c+1)\theta} (\sin \theta)^c (\cos \theta)^{c-1} {}_3F_2 \left[\begin{matrix} a, b, d+1 \\ a+b+1, d \end{matrix} ; e^{i\theta} \cos \theta \right] d\theta = e^{i\frac{\pi}{2}(c+1)} \frac{\Gamma(c)\Gamma(c+1)}{\Gamma(2c+1)} s_1 \tag{6}$$

provided $d \notin \mathbb{Z}_0^-$, $Re(c) > 0$, $Re(2c - a - b) > -2$ and s_1 is the same as given in (4).

Proof:

To derive result (6) stated in Theorem 6, we follow the approach outlined below. Let Π represent the left-hand side of equation (6), we have

$$I = \int_0^{\frac{\pi}{2}} e^{i(2c+1)\theta} (\sin \theta)^c (\cos \theta)^{c-1} \times {}_3F_2 \left[\begin{matrix} a, b, d+1 \\ \frac{a+b+1}{2}, d \end{matrix} ; e^{i\theta} \cos \theta \right] d\theta$$

Expressing the generalized hypergeometric function ${}_3F_2$ as a series, we have

$$I = \int_0^{\frac{\pi}{2}} e^{i(2c+1)\theta} (\sin \theta)^c (\cos \theta)^{c-1} \times \sum_{n=0}^{\infty} \frac{(a)_n (b)_n (d+1)_n}{\left(\frac{a+b+1}{2}\right)_n (d)_n} \cdot \frac{e^{in\theta} (\cos \theta)^n}{n!} d\theta$$

Rearranging the order of integration and summation is justified by the uniform convergence of the series and the absolute convergence of the integral, we have

$$I = \sum_{n=0}^{\infty} \frac{(a)_n (b)_n (d+1)_n}{\left(\frac{a+b+1}{2}\right)_n (d)_n} \cdot \frac{1}{n!} \times \int_0^{\frac{\pi}{2}} e^{i(2c+n+1)\theta} (\sin \theta)^c (\cos \theta)^{c+n-1} d\theta$$

Evaluating the integral with the help of the known integral (5) due to MacRobert, we have

$$I = \sum_{n=0}^{\infty} \frac{(a)_n (b)_n (d+1)_n}{\left(\frac{a+b+1}{2}\right)_n (d)_n} \times e^{\frac{i\pi}{2}(c+1)} \frac{\Gamma(c+1)\Gamma(c+n)}{\Gamma(2c+n+1)}$$

After a little simplification, we have

$$I = e^{\frac{i\pi}{2}(c+1)} \frac{\Gamma(c)\Gamma(c+1)}{\Gamma(2c+1)} \sum_{n=0}^{\infty} \frac{(a)_n (b)_n (c)_n (d+1)_n}{\left(\frac{a+b+1}{2}\right)_n (2c+1)_n (d)_n n!}$$

Summing up the series, we have

$$I = e^{\frac{i\pi}{2}(c+1)} \frac{\Gamma(c)\Gamma(c+1)}{\Gamma(2c+1)} {}_4F_3 \left[\begin{matrix} a, b, c, d+1 \\ \frac{a+b+1}{2}, 2c+1, d \end{matrix} ; 1 \right]$$

We can now see that the ${}_4F_3$ can be evaluated using the known result (4), leading us to the right-hand side of equation (6). This concludes the proof of result (6) stated in the theorem.

We conclude this section by noting that in the following section, we will present several interesting special cases of our main results.

3. Special Cases

In this section, we shall mention a few special cases of our main findings.

Corollary 3.1

In (6), If we take $d = 2c$, then we get the following interesting results:

$$\int_0^{\frac{\pi}{2}} e^{i(2c+1)\theta} (\sin \theta)^c (\cos \theta)^{c-1} {}_3F_2 \left[\begin{matrix} a, b, 2c+1 \\ \frac{a+b+1}{2}, 2c \end{matrix} ; e^{i\theta} \cos \theta \right] d\theta = e^{\frac{i\pi}{2}(c+1)} \frac{\Gamma(c)\Gamma(c+1)}{\Gamma(2c+1)} s \quad (7)$$

provided $R(c) > 0$, $Re(2c - a - b) > -1$ and s is the same as given in (2).

Corollary 3.2

In (6), first we let $b = -2n$ and replace a by $a + 2n$ and we let $b = -2n - 1$ and replace a by $a + 2n + 1$, where n is zero or a positive integer. In both cases, one of the two terms appearing on the right-hand side of the resulting integral (6) vanishes and we get the following interesting results:

$$\begin{aligned} & \int_0^{\frac{\pi}{2}} e^{i(2c+1)\theta} (\sin \theta)^c (\cos \theta)^{c-1} {}_3F_2 \left[\begin{matrix} -2n, a+2n, d+1 \\ \frac{a+1}{2}, d \end{matrix} ; e^{i\theta} \cos \theta \right] d\theta \\ &= e^{\frac{i\pi}{2}(c+1)} \frac{\Gamma(c)\Gamma(c+1)}{\Gamma(2c+1)} \frac{\left(\frac{1}{2}\right)_n \left(\frac{a}{2} - c + \frac{1}{2}\right)_n}{\left(\frac{a}{2} + \frac{1}{2}\right)_n \left(c + \frac{1}{2}\right)_n} \end{aligned} \quad (8)$$

The beauty of this result is that the right-hand side of (8) is independent of d .

And

$$\begin{aligned} & \int_0^{\frac{\pi}{2}} e^{i(2c+1)\theta} (\sin \theta)^c (\cos \theta)^{c-1} {}_3F_2 \left[\begin{matrix} -2n-1, a+2n+1, d+1 \\ \frac{a+1}{2}, d \end{matrix} ; e^{i\theta} \cos \theta \right] d\theta \\ &= \frac{e^{\frac{i\pi}{2}(c+1)}}{\Gamma(2c+1)} \left(1 - \frac{2c}{d}\right) \frac{\Gamma(c)\Gamma(c+1)}{\Gamma(2c+1)} \frac{\left(\frac{3}{2}\right)_n \left(\frac{a}{2} - c + \frac{1}{2}\right)_n}{\left(\frac{a}{2} + \frac{1}{2}\right)_n \left(c + \frac{3}{2}\right)_n} \end{aligned} \quad (9)$$

Corollary 3.3

In (9), if we take $d = 2c$, we get the following elegant result

$$\int_0^{\frac{\pi}{2}} e^{i(2c+1)\theta} (\sin \theta)^c (\cos \theta)^{c-1} \times {}_3F_2 \left[\begin{matrix} -2n-1, & a+2n+1, & 2c+1 \\ & \frac{a+1}{2}, & 2c \end{matrix} ; e^{i\theta} \cos \theta \right] d\theta = 0 \quad (10)$$

Similarly, other results can be obtained.

4. Conclusion

In this paper, we explored an integral representation involving the generalized hypergeometric function, shedding light on its utility and significance in mathematical analysis. We conclude this paper by remarking that in 2016, Choi and Rathie [3] established thirteen results for the series ${}_4F_3$ [1]. Other results similar to what we have obtained in this paper are under investigation and will form a part of the subsequent paper in this direction. Their contributions provide a foundational basis for examining related functions and their integrals in greater depth.

References

- [1] Bailey, W. N. (1964). Generalized Hypergeometric Series, Cambridge: *Cambridge University Press*, 1935; Reprinted by *Stechert-Hafner*, New York (1964).
- [2] Basnet, G. B., Pahari, N. P. & Poudel, M. P. (2024) . A result on an integral involving product of two generalized hypergeometric functions and its applications, *Journal of Nepal Mathematical Society (JNMS)*, **7(2)**: 22-29.
- [3] Choi, J. & Rathie, A. K. (2016). Certain new summation formulas for the series ${}_4F_3(1)$ with applications, *J. Nonlinear Sci. Appl.*, **9**: 4722-4736.
- [4] Kim, Y. S., Rakha, M. A. & Rathie, A. K. (2010). Extension of certain classical summation theorems for the series ${}_2F_1$, ${}_3F_2$, and ${}_4F_3$ with applications in Ramanujan's summations, *Int. J. Math.Sci*, Article ID 309503, 26 pages.
- [5] Lavoie, J. L., Grondm, F. & Rathie, A. K. (1992). Generalization of Watson's theorem on the sum of a ${}_3F_2$, *Indian J. Math*, **34**: 23 - 32.
- [6] MacRobert, T. M. (1961). Beta Function formula and integrals involving E - Function, *Math. Anallen*, **142**: 450-452.
- [7] Poudel, M. P., Pahari, N. P., Basnet, G.B. & Poudel, R. P. (2023). Connection Formulas on Kummer's Solutions and their Extension on Hypergeometric Function. *Nepal Journal of Mathematical Sciences*, **4(2)**: 83-88
- [8] Rainville, E. D. (1960). *Special Functions*, New York: MacMillan Company, 1960.

□□



Nepal Journal of Mathematical Sciences (NJMS)
ISSN: 2738-9928 (online), 2738-9812 (print)
Vol. 5, No. 1, 2024 (February): 7-14
DOI: <https://doi.org/10.3126/njmathsci.v5i1.76442>
©School of Mathematical Sciences,
Tribhuvan University, Kathmandu, Nepal

Research Article
Received Date: December 7, 2024
Accepted Date: February 12, 2025
Published Date: February 28, 2025

Study of Common Fixed Point Theorems for Interpolative Contraction in Metric Space

Surendra Kumar Tiwari^{1*} & Jayant Prakash Ganvir²

^{1,2}Department of Mathematics, Dr. C. V. Raman University, Bilaspur, India

Corresponding Author: *sk10tiwari@gmail.com

Abstract: This paper aims to establish common fixed point results that can be addressed using an interpolative contraction condition proposed by Karapinar et al. [6] and Karapinar et al. [7] within a complete metric space. We have developed both the H-R type contraction and R-R-C-Rus-type contraction in the context of metric spaces, and we have proved related interpolation common fixed point theorem. Furthermore, we provide examples to illustrate the significance of our findings.

Keywords: Metric space, Common fixed point, Interpolation, Hardy–Rogers contraction, Reich–Rus–Ćirić contraction.

1. Introduction and preliminaries

The Banach contraction mapping principle (BCP) was developed by the Polish mathematician Stefan Banach [1] in 1922 and focuses on contraction mappings with unique fixed point results on metric spaces. Due to its importance, several authors have extended and generalized this principle. Researchers have been inspired to explore alternative forms of contraction based on Banach's FPT. A notable early response came from Kannan [2, 3] in 1968 and 1969, who introduced a new type of contraction mapping that does not require continuity.

Definition 1.1(see [2, 3]): A mapping $\mathcal{G}: \mathcal{W} \rightarrow \mathcal{W}$ is called Kannan type contraction, if there exists $\mathcal{k} \in [0, \frac{1}{2})$ such that

$$d(\mathcal{G}p, \mathcal{G}q) \leq \mathcal{k}[d(p, \mathcal{G}p) + d(q, \mathcal{G}q)] \text{ for all } p, q \in \mathcal{W}. \quad (1)$$

Kannan [2, 3] established the following theorem:

Theorem 1.2 (see [2, 3]): If (\mathcal{W}, d) is a complete metric space, then every Kannan contraction on \mathcal{W} has a unique fixed point.

A notable recent generalization of the Kannan theorem was published by Karapinar E. [4] in 2018. He presented a new type of contraction obtained from interpolation of the Kannan contraction as follows:

Definition 1.3 (see [4]): A mapping $\mathcal{G}: \mathcal{W} \rightarrow \mathcal{W}$ is called interpolative Kannan type contraction on metric space (\mathcal{W}, d) , if there exists $\mathcal{k} \in [0, \frac{1}{2})$ such that

$$d(\mathcal{G}p, \mathcal{G}q) \leq \mathcal{k}[d(p, \mathcal{G}p)]^\alpha [d(q, \mathcal{G}q)]^{1-\alpha} \text{ for all } p, q \in \mathcal{W} \text{ with } p \neq \mathcal{G}p \text{ and } q \neq \mathcal{G}q. \quad (2)$$

Karapinar, E. [4] established the following theorem:

Theorem 1.4 (see [4]): If (\mathcal{W}, d) is a complete metric space, then every interpolative Kannan type contraction on \mathcal{W} has unique fixed point.

However, the theorem 1.4 has been generalized by Noorwali [15] who obtained a common fixed point for two maps as follows:

Theorem 1.5: Suppose (\mathcal{W}, d) be a metric space and $\mathcal{G}, \mathcal{H}: \mathcal{W} \rightarrow \mathcal{W}$ be self mappings. Take over that $\exists \sigma \in [0,1)$ and $\alpha \in (0,1)$ with $\alpha + \beta + \gamma < 1$, satisfied the condition

$$d(\mathcal{G}a, \mathcal{H}b) \leq \sigma [d(a, \mathcal{G}a)]^\alpha \cdot [d(b, \mathcal{H}b)]^{1-\alpha} \quad (3)$$

for all $a, b \in \mathcal{W}$ such that $\mathcal{G}a \neq a$ whenever $\mathcal{H}b \neq b$. Then \mathcal{G} and \mathcal{H} have a unique common fixed point.

In sequel, Karapinar, et al. [6] introduced the notion of interpolative Hardy- Rogers's type contraction by using the well known contraction of Hardy and Rogers [5].

Definition1.5 (see [6]): A self-mapping $\mathcal{G}: \mathcal{W} \rightarrow \mathcal{W}$ is called an interpolative H-R type contraction metric space (\mathcal{W}, d) , if $\exists \mathcal{k} \in [0,1)$ and $\alpha, \beta, \gamma \in (0,1)$ where $\alpha + \beta + \gamma < 1$, such that

$$d(\mathcal{G}p, \mathcal{G}q) \leq \mathcal{k} [d(p, q)]^\beta \cdot [d(p, \mathcal{G}p)]^\alpha \cdot [d(q, \mathcal{G}q)]^\gamma \cdot \left[\frac{1}{2} (d((p, \mathcal{G}q) + d(q, \mathcal{G}p)) \right]^{1-\alpha-\beta-\gamma} \quad (4)$$

for all $p, q \in \mathcal{W} \setminus \text{Fix}(\mathcal{G})$.

Karpinar et al. [6] established the following theorem:

Theorem 1.6 (see [6]): Let (\mathcal{W}, d) be a complete metric space and \mathcal{G} be an interpolative Hardy-Rogers type contraction. In that case, \mathcal{G} is fixed point of \mathcal{W} .

Very recently, Karapinar et al. [7] introduced the notion of Interpolative Riech-Rus- Ciric type contraction by using the well known contraction of Riech-Rus-Ciric [8-14].

Definition 1.7 (see [7]): Let (\mathcal{W}, d) be a metric space. Then a self mapping $\mathcal{G}: \mathcal{W} \rightarrow \mathcal{W}$ is called interpolative Riech-Rus-Ciric type contraction if there exists $\mathcal{k} \in [0; 1)$, $\alpha_1, \alpha_2 \in [0,1)$ with $\alpha_1 + \alpha_2 < 1$ such that

$$d(\mathcal{G}p, \mathcal{G}q) \leq \mathcal{k} [d(p, q)]^\alpha \cdot [d(p, \mathcal{G}p)]^{\alpha_2} \cdot [d(q, \mathcal{G}q)]^{1-\alpha_2-\alpha_3} \quad \text{for all } p, q \in \mathcal{W}. \quad (5)$$

Karapinar et al. [7] proved the following theorem

Theorem 1.8 (see [7]): Let (\mathcal{W}, d) be a complete metric space and \mathcal{G} be an interpolative Reich-Rush-Ciric type contraction. In that case, \mathcal{G} is fixed point of \mathcal{W} .

Very Recently, Zahid et al. [16] introduced Reich-Rus-Ciric type contraction in rectangular \mathcal{M} -metric spaces and obtained fixed point theorems in these spaces. In the same year, Edraoui M. et al. [17] presented some fixed point results of Hardy-Rogers-type for cyclic mappings on complete metric space. Later, many authors continued their investigations and more results were obtained, such as, [18-27].

2. Main Result

In this section, we extend and generalize the result of Karapinar et al. [6] of theorem 1.6 and Karapinar et al. [7] of theorem 1.8 to obtain common fixed point results. First, we extend the theorem 1.6 as follows:

Theorem 2.1: Suppose $\mathcal{G}, \mathcal{H}: \mathcal{W} \rightarrow \mathcal{W}$ be any two self-interpolative Hardy- Rogers type contraction on metric space (\mathcal{W}, d) and if $\exists r \in [0,1)$ and $\alpha, \beta, \gamma \in (0,1)$ while $\alpha + \beta + \gamma < 1$, satisfied the condition by definition 1.5

$$d(\mathcal{G}a, \mathcal{H}b) \leq r [d(a, b)]^\beta \cdot [d(a, \mathcal{G}a)]^\alpha \cdot [d(b, \mathcal{H}b)]^\gamma \cdot \left[\frac{1}{2} (d(a, \mathcal{H}b) + d(b, \mathcal{G}a)) \right]^{1-\alpha-\beta-\gamma} \quad (6)$$

for all $a, b \in \mathcal{W}$ such that $\mathcal{G}a \neq a$ whenever $\mathcal{H}b \neq b$. Then \mathcal{G} and \mathcal{H} have a unique common fixed point.

Proof:

Consider $a_0 \in \mathcal{W}$ with sequence $\{a_{2\eta}\}$ such as

$$a_{2\eta+1} = \mathcal{G}a_{2\eta} \text{ and } a_{2\eta+2} = \mathcal{H}a_{2\eta+1}, \forall \eta \in \{0,1,2, \dots\}.$$

Even if $\exists \eta \in \{0,1,2, \dots\}$ and $a_{2\eta} = a_{2\eta+1} = a_{2\eta+2}$, also, $a_{2\eta}$ is a common fixed point of \mathcal{G} and \mathcal{H} , so let us suppose that there does not exist three consecutive identical terms in the sequence $\{a_{2\eta}\}$ and that $a_0 \neq a_1$.

By substituting the values $a = a_{2\eta}$ and $b = a_{2\eta+1}$ in (6), we get

$$\begin{aligned} d(a_{2\eta+1}, a_{2\eta+2}) &= d(\mathcal{G}a_{2\eta}, \mathcal{H}a_{2\eta+1}) \\ &\leq r [d(a_{2\eta}, a_{2\eta+1})]^\beta \cdot [d(a_{2\eta}, \mathcal{G}a_{2\eta})]^\alpha \cdot [d(a_{2\eta+1}, \mathcal{H}a_{2\eta+1})]^\gamma \cdot \\ &\quad \left[\frac{1}{2} (d(a_{2\eta}, \mathcal{H}a_{2\eta+1}) + d(a_{2\eta+1}, \mathcal{G}a_{2\eta})) \right]^{1-\alpha-\beta-\gamma} \\ &\leq r [d(a_{2\eta}, a_{2\eta+1})]^\beta \cdot [d(a_{2\eta}, a_{2\eta+1})]^\alpha \cdot [d(a_{2\eta+1}, a_{2\eta+2})]^\gamma \cdot \\ &\quad \left[\frac{1}{2} (d(a_{2\eta}, a_{2\eta+2}) + d(a_{2\eta+1}, a_{2\eta+1})) \right]^{1-\alpha-\beta-\gamma} \\ &\leq r [d(a_{2\eta}, a_{2\eta+1})]^\beta \cdot [d(a_{2\eta}, a_{2\eta+1})]^\alpha \cdot [d(a_{2\eta+1}, a_{2\eta+2})]^\gamma \cdot \\ &\quad \left[\frac{1}{2} (d(a_{2\eta}, a_{2\eta+1}) + d(a_{2\eta+1}, a_{2\eta+2})) \right]^{1-\alpha-\beta-\gamma}. \end{aligned} \quad (7)$$

Suppose that $d(a_{2\eta}, a_{2\eta+1}) < d(a_{2\eta+1}, a_{2\eta+2})$, for $r \geq 1$.

Thus

$$\left[\frac{1}{2} (d(a_{2\eta}, a_{2\eta+1}) + d(a_{2\eta+1}, a_{2\eta+2})) \right] \leq d(a_{2\eta+1}, a_{2\eta+2}).$$

Consequently, the inequality (7), yields that

$$[d(a_{2\eta+1}, a_{2\eta+2})]^{\beta+\gamma} \leq r [d(a_{2\eta}, a_{2\eta+1})]^{\beta+\gamma}. \quad (8)$$

So, we conclude that $d(a_{2\eta}, a_{2\eta+1}) \geq d(a_{2\eta+1}, a_{2\eta+2})$, which is conflict. Accordingly

$$d(a_{2\eta+1}, a_{2\eta+2}) \leq d(a_{2\eta}, a_{2\eta+1}) \forall r \geq 1.$$

Where, $d(a_{2\eta}, a_{2\eta+1})$ is a positive term and non increasing sequence. Consequently a non negative constant ℓ such as $\lim_{\eta \rightarrow \infty} d(a_{2\eta}, a_{2\eta+1}) = \ell$.

We have

$$\left[\frac{1}{2} d(a_{2\eta}, a_{2\eta+1}) + d(a_{2\eta+1}, a_{2\eta+2}) \right] \leq d(a_{2\eta}, a_{2\eta+1}), \text{ for all } \eta \geq 1.$$

By the inequality (7), we get

$$[d(a_{2\eta+1}, a_{2\eta+2})]^{1-\alpha} \leq r[d(a_{2\eta}, a_{2\eta+1})]^{1-\alpha}, \text{ for all } \eta \geq 1. \tag{9}$$

We deduce that

$$d(a_{2\eta+1}, a_{2\eta+2}) \leq r d(a_{2\eta}, a_{2\eta+1}) \leq \dots \leq r^{2\eta} d(a_0, a_1) \tag{10}$$

Now using (10), and claim that $\{a_{2\eta}\}$ having Cauchy sequence. Let $\eta, \ell \in \{0, 1, 2, \dots\}$

$$\begin{aligned} d(a_{2\eta}, a_{2\eta+2\ell}) &\leq d(a_{2\eta}, a_{2\eta+1}) + d(a_{2\eta+1}, a_{2\eta+2}) + \dots + d(a_{2\eta+2\ell-1}, a_{2\eta+2\ell}) \\ &\leq [r^{2\eta} + r^{2\eta+1} + \dots + r^{2\eta+2\ell-1}] d(a_0, a_1) \\ &\leq \frac{r^{2\eta}}{1-r} d(a_0, a_1). \end{aligned} \tag{11}$$

Letting $\eta \rightarrow \infty$, we deduce that $\{a_{2\eta}\}$ is a Cauchy sequence in the complete metric space (\mathcal{W}, d) and $\exists u \in \mathcal{W}$ such that

$$\lim_{\eta \rightarrow \infty} a_{2\eta} = u.$$

Now, prove that u is a common fixed point of \mathcal{G} and \mathcal{H} . Now consider,

$$\begin{aligned} d(\mathcal{G}u, a_{2\eta+2}) &= d(\mathcal{G}u, \mathcal{H}a_{2\eta+1}) \\ &\leq r [d(u, a_{2\eta+1})]^\beta \cdot [d(u, \mathcal{G}u)]^\alpha \cdot [d(a_{2\eta+1}, \mathcal{H}a_{2\eta+1})]^\gamma. \\ &\quad \left[\frac{1}{2} (d(a_{2\eta+1}, \mathcal{G}u) + d(a_{2\eta+1}, a_{2\eta+2})) \right]^{1-\alpha-\beta-\gamma}. \end{aligned}$$

Letting $\eta \rightarrow \infty$, we get $d(\mathcal{G}u, u) = 0 \Rightarrow \mathcal{G}u = u$.

Similarly, we can prove that $\mathcal{H}u = u$. Since $\mathcal{G}u = u = \mathcal{H}u$. Hence, u is a common fixed point of \mathcal{G} and \mathcal{H} .

Now, we claim that u is the unique common fixed point theorem of \mathcal{G} and \mathcal{H} . Suppose that v is another common fixed point of \mathcal{G} and \mathcal{H} , then

$$\begin{aligned} d(u, v) &= d(\mathcal{G}u, \mathcal{H}v) \\ &\leq r [d(u, v)]^\beta \cdot [d(u, \mathcal{G}u)]^\alpha \cdot [d(v, \mathcal{H}v)]^\gamma \cdot \left[\frac{1}{2} (d(u, \mathcal{H}v) + d(v, \mathcal{G}u)) \right]^{1-\alpha-\beta-\gamma} \\ &= 0. \end{aligned}$$

Hence $u = v$. Thus, u is the unique common fixed point theorem of \mathcal{G} and \mathcal{H} .

Example 2.2: Consider $\mathcal{W} = \{0, 1, 2, 3, 5\}$ endowed with $d(a, b) = |a - b|$.

Now let

$$\alpha = \frac{1}{3}, \quad \beta = \frac{1}{2} \quad \text{and} \quad \gamma = \frac{1}{7}.$$

It is obvious that

$$d(\mathcal{G}a, \mathcal{G}b) \leq r [d(a, b)]^\beta \cdot [d(a, \mathcal{G}a)]^\alpha \cdot [d(b, \mathcal{H}b)]^\gamma \cdot \left[\frac{1}{2} (d((a, \mathcal{H}b)) + d(b, \mathcal{G}a)) \right]^{1-\alpha-\beta-\gamma}$$

for all $a, b \in \mathcal{W}$ such that $\mathcal{G}a \neq a$ whenever $\mathcal{H}b \neq b$, that is (7) hold.

All the hypotheses of Theorem 2.1 are satisfied, and so 0 and 1 are common fixed points.

Next, we will extend and generalize the Theorem 1.8 as follows:

Theorem 2.3: Suppose $\mathcal{G}, \mathcal{H}: \mathcal{W} \rightarrow \mathcal{W}$ be any two self-interpolative R-R-C type contraction metric space (\mathcal{W}, d) and satisfied the condition by definition 1.7, if $\exists t \in [0, 1)$ with $\alpha_1, \alpha_2 \in (0, 1)$ where $\alpha_1 + \alpha_2 < 1$, such that

$$d(\mathcal{G}a, \mathcal{H}b) \leq t [d(a, b)]^{\alpha_1} \cdot [d(a, \mathcal{G}a)]^{\alpha_2} \cdot [d(b, \mathcal{H}b)]^{1-\alpha_1-\alpha_2} \quad (12)$$

for all $a, b \in \mathcal{W}$ such that $\mathcal{G}a \neq a$ whenever $\mathcal{H}b \neq b$. Then \mathcal{G} and \mathcal{H} have a unique common fixed point.

Proof:

Consider $a_0 \in \mathcal{W}$ with sequence $\{a_{2\eta}\}$ such as

$$a_{2\eta+1} = \mathcal{G}a_{2\eta} \text{ and } a_{2\eta+2} = \mathcal{H}a_{2\eta+1}, \forall \eta \in \{0, 1, 2, \dots\}.$$

Since $\eta \in \{0, 1, 2, \dots\}$ and $a_{2\eta} = a_{2\eta+1} = a_{2\eta+2}$, hence $a_{2\eta}$ is a common fixed point of \mathcal{G} and \mathcal{H} , so let us suppose that there does not exist $a_0 \neq a_1$.

By substituting the values $a = a_{2\eta}$ and $b = a_{2\eta+1}$ in (12), we get

$$\begin{aligned} d(a_{2\eta+1}, a_{2\eta+1}) &= d(\mathcal{G}a_{2\eta}, \mathcal{H}a_{2\eta+1}) \\ &\leq t [d(a_{2\eta}, a_{2\eta+1})]^{\alpha_1} \cdot [d(a_{2\eta}, \mathcal{G}a_{2\eta})]^{\alpha_2} \cdot [d(a_{2\eta+1}, \mathcal{H}a_{2\eta+1})]^{1-\alpha_1-\alpha_2} \\ &\leq t [d(a_{2\eta}, a_{2\eta+1})]^{\alpha_1} \cdot [d(a_{2\eta}, a_{2\eta+1})]^{\alpha_2} [d(a_{2\eta+1}, a_{2\eta+2})]^{1-\alpha_1-\alpha_2} \end{aligned}$$

This implies that

$$[d(a_{2\eta+1}, a_{2\eta+2})]^{\alpha_1+\alpha_2} \leq t [d(a_{2\eta}, a_{2\eta+1})]^{\alpha_1+\alpha_2}$$

or

$$d(a_{2\eta+1}, a_{2\eta+2}) \leq t d(a_{2\eta}, a_{2\eta+1})$$

Hence

$$d(a_{2\eta+1}, a_{2\eta+2}) \leq t d(a_{2\eta}, a_{2\eta+1}) \leq \dots \dots \leq t^{2\eta} d(a_0, a_1) \dots \quad (13)$$

Similarly, we can show that

$$[d(a_{2\eta+1}, a_{2\eta})]^{1-\alpha_2} \leq t [d(a_{2\eta}, a_{2\eta-1})]^{1-\alpha_2}$$

or

$$[d(a_{2\eta+1}, a_{2\eta})] \leq t [d(a_{2\eta}, a_{2\eta-1})].$$

Hence $d(a_{2\eta+1}, a_{2\eta}) \leq t d(a_{2\eta-1}, a_{2\eta}) \leq \dots \dots \leq t^{2\eta} d(a_0, a_1) \dots \quad (14)$

From (13) and (14), we can deduce that

$$d(a_{2\eta}, a_{2\eta+1}) \leq t^{2\eta} d(a_0, a_1) \quad (15)$$

Now using (15), and show that $\{a_{2\eta}\}$ is a Cauchy sequence. Let $\eta, \ell \in \{0,1,2, \dots\}$, we have

$$\begin{aligned} d(a_{2\eta}, a_{2\eta+2\ell}) &\leq d(a_{2\eta}, a_{2\eta+1}) + d(a_{2\eta+1}, a_{2\eta+2}) + \dots + d(a_{2\eta+2\ell-1}, a_{2\eta+2\ell}) \\ &\leq [t^{2\eta} + t^{2\eta+1} + \dots + t^{2\eta+2\ell-1}]d(a_0, a_1) \\ &\leq \frac{t^{2\eta}}{1-t} d(a_0, a_1). \end{aligned} \tag{16}$$

Letting $\eta, \ell \rightarrow \infty$, i.e $\lim_{\eta, \ell \rightarrow \infty} d(a_{2\eta}, a_{2\eta+2\ell}) = 0$.

Therefore, $\{a_{2\eta}\}$ is a Cauchy sequence in (\mathcal{W}, d) and $\exists \tau \in \mathcal{W}$ such that

$$\lim_{\eta \rightarrow \infty} a_{2\eta} = \tau.$$

Now consider,

$$\begin{aligned} d(\mathcal{G}\tau, a_{2\eta+2}) &= d(\mathcal{G}\tau, \mathcal{H}a_{2\eta+1}) \\ &\leq t[d(\tau, a_{2\eta+1})]^{\alpha_1}. [d(\tau, \mathcal{G}\tau)]^{\alpha_2}. [d(a_{2\eta+1}, \mathcal{H}a_{2\eta+1})]^{1-\alpha_1-\alpha_2}. \end{aligned}$$

Letting $\eta \rightarrow \infty$, we get $d(\mathcal{G}\tau, \tau) = 0 \Rightarrow \mathcal{G}\tau = \tau$.

Similarly, $d(a_{2\eta+1}, \mathcal{H}\tau) = d(\mathcal{G}a_{2\eta}, \mathcal{H}\tau)$

$$\leq t[d(a_{2\eta}, \mathcal{H}\tau)]^{\alpha_1}. [d(a_{2\eta}, \mathcal{H}a_{2\eta})]^{\alpha_2}. [d(\tau, \mathcal{H}\tau)]^{1-\alpha_1-\alpha_2}.$$

Letting $\eta \rightarrow \infty$, we get $d(\tau, \mathcal{H}\tau) = 0$, hence $\mathcal{H}\tau = \tau$.

Since $\mathcal{G}\tau = \tau = \mathcal{H}\tau$. So, τ is common fixed point of \mathcal{G} and \mathcal{H} .

Next, we show that, common fixed point τ is the unique of \mathcal{G} and \mathcal{H} . Suppose that, ς is another common fixed point of \mathcal{G} and \mathcal{H} , then

$$\begin{aligned} d(\tau, \varsigma) &= d(\mathcal{G}\tau, \mathcal{H}\varsigma) \\ &\leq t[d(\tau, \varsigma)]^{\alpha_1}. [d(\tau, \mathcal{G}\tau)]^{\alpha_2}. [d(\varsigma, \mathcal{H}\varsigma)]^{1-\alpha_1-\alpha_2}. \\ &= 0. \end{aligned}$$

Hence $\tau = \varsigma$. As follows, common fixed point τ is a unique of \mathcal{G} and \mathcal{H} .

If we take $\alpha_1 = 0$ in Theorem 2.3, then we get the following Corollary

Corollary 2.4: Suppose $\mathcal{G}, \mathcal{H}: \mathcal{W} \rightarrow \mathcal{W}$ be any two self-interpolative R-R-C type contraction metric space (\mathcal{W}, d) and satisfied the condition by definition 1.7, if $\exists t \in [0,1)$ with $\alpha_1, \alpha_2 \in (0,1)$ where $\alpha_1 + \alpha_2 < 1$, such that

$$d(\mathcal{G}a, \mathcal{H}b) \leq t[d(a, \mathcal{G}a)]^{\alpha_2}. [d(b, \mathcal{H}b)]^{1-\alpha_2} \tag{17}$$

for all $a, b \in \mathcal{W}$ such that $\mathcal{G}a \neq a$ whenever $\mathcal{H}b \neq b$. Accordingly, \mathcal{G} and \mathcal{H} have a unique common fixed point.

Example 2.5: Consider $\mathcal{W} = \{1,2,3,4\}$.and $d(a, b) = \max\{a, b\} + |a - b|$ that is

$d(a, b)$	1	2	3	4
1	1	3	5	7
2	3	2	4	6
3	5	4	3	5
4	7	6	5	4

Now, a self mappings of \mathcal{G} and \mathcal{H} on \mathcal{W} as

$$\mathcal{G} = \begin{pmatrix} 1 & 2 & 3 & 4 \\ 1 & 2 & 1 & 2 \end{pmatrix} \text{ and } \mathcal{H} = \begin{pmatrix} 1 & 2 & 3 & 4 \\ 1 & 2 & 2 & 1 \end{pmatrix} \text{ as shown in Figure 1.}$$

Choose $\alpha_1 = \frac{1}{2}$, $\alpha_2 = \frac{1}{3}$ and $t = \frac{7}{10}$.

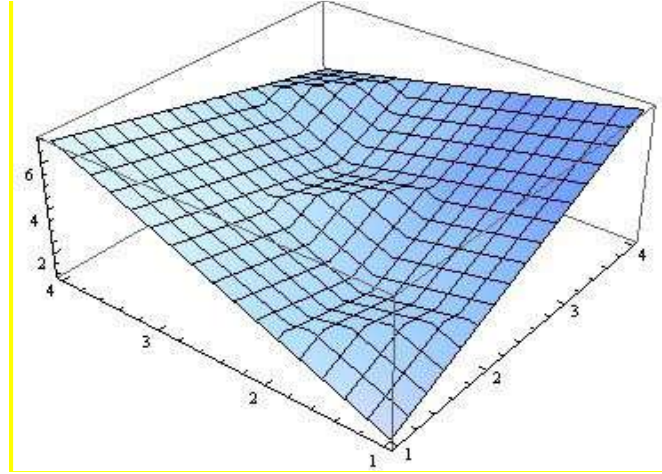


Figure1. 1 is the common fixed point of \mathcal{G} and \mathcal{H} .

Case 1. Presume $(a, b) = (3, 4)$, we have

$$\begin{aligned} d(\mathcal{G}a, \mathcal{H}b) &\leq t[d(a, b)]^{\alpha_1} \cdot [d(a, \mathcal{G}a)]^{\alpha_2} \cdot [b, \mathcal{H}b]^{1-\alpha_1-\alpha_2} \\ d(\mathcal{G}3, \mathcal{H}4) &= 1 \\ &\leq t[d(3, 4)]^{1/3} \cdot [d(3, \mathcal{G}3)]^{1/2} \cdot [4, \mathcal{H}4]^{1/6}. \end{aligned}$$

Case 2. Let $(a, b) = (1, 4)$, $d(\mathcal{G}1, \mathcal{H}4) = 1$

$$\leq t[d(1, 4)]^{1/3} \cdot [d(1, \mathcal{G}1)]^{1/2} \cdot [4, \mathcal{H}4]^{1/6}.$$

Therefore, 1 is the common fixed point of \mathcal{G} and \mathcal{H} in the setting of the interpolative R-R-C type contraction.

3. Conclusion

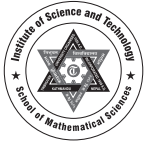
This article examines a significant contraction that demonstrates a unique common fixed point for both the Interpolative H-R contraction and the Interpolative R-R-C type contraction mappings within a metric space. Our main results build upon and extend the earlier research conducted by Karapinar et al. [6] and Karapinar et al. [7]. Furthermore, we present a relevant example to support these findings.

References

- [1] Banach, S. (1922). Sur les opérations dans les ensembles abstraits et leur applications aux équations intégrales. *Fund. Math.*, **3**: 133-181.
- [2] Kannan, R. (1968). Some results on fixed points. *Bull. Calcutta, Math. Soc.*, **60**: 71-76.
- [3] Kannan, R. (1969). Some results on fixed points-II. *A. M. Math. Mon.*, **76**: 405-408.
- [4] Karapinar, E. (2018). Revisiting the Kannan type contractions via interpolation. *Advances in the Theory on Non linear Analysis and its Applications*, **2(2)**: 85-87.
- [5] Hardy G. E. & Rogers T.D. (1973). A generalization of a fixed point theorem of Reich Can. *Math. Bull.* **16**: 201-206.
- [6] Karapinar, E., Alqahtani, O. & Aydi H. (2018). On interpolative Hardy –Rogers type contractions. *Symmetry*. **11**: 1-7.

- [7] Karapinar, E., Agrawal R.P. & Aydi H. (2019). Interpolative Reich- Rus- Ciric type Contraction on partial metric space. *Mathematics*. **6(256)**: 1-7.
- [8] Reich, S. (1972). Fixed point of contractive function, *Bolletino Dell Union Mathemaica Italiana*. **4**: 26-62.
- [9] Reich, S.(1971). Some remarks concerning contraction mappings. *Can. Math. Bull.* 14, 121-124.
- [10] Reich S. (1971). Kannan fixed point theorem. *Boll. Dell Unione. Mat. Ital.*, 41-11.
- [11] Ciric, L. B. (1971). On contraction type mapping, *Math. Balk*, **1**: 52-57.
- [12] Ciric, L.B., (1971). Generalized contractions and fixed point theorems. *Publ. Inst. Math. (Beograd,)*. **12**: 19- 26.
- [13] Rus, I.A. (2001). *Generalized Contractions and Applications*. Cluj University Press: Clui- Napoca, Romania, 2001.
- [14] Rus, I.A. (1979). *Principles and Applications of the Fixed Point Theory*. Editura Dacia, Clui. Napoca, Romani (In Romanian).
- [15] Noorwali, M. (2018). Common fixed point for Kannan type Contraction via Interpolation, *Journal of Mathematical Analysis*, **9(6)**: 92-94.
- [16] Zahid, M. ,Raza A., & Khan S. H. (2024). Some innovative results for interpolative Reich-Rus- Ciric- type contraction rectangular M –metric spaces, *Axiom*, **13**: 1-20.
- [17] M., Koufi El., & Aamri M. (2024). On interpolative Hardy-Rogers type cyclic contractions, *Appl. Gen. Topol.*, **25(1)**: 117-124.
- [18] Edraoui, M., Aamri M., & Lazaiz S. (2020). Fixed point theorem for α non- expansiv wrt orbits in locally convex space, *J. Math. Comput. Sci.*, **10**: 1582-1589.
- [19] Edraoui M., Koufi A. El., & Semami, S. (2023). Fixed points results for Various types of interpolative cyclic contraction, *Appl. Gen. Topol.* . **24 (2)**: 247-252.
- [20] Bekri Y. El., Edraoui M., Mouline J., & Bassou A.(2023). Interpolative Ciric-Reich- Rus type contraction in G-metric spaces, *Journal of Survey in Fisheries Sciences*.(**3**): 17- 20.
- [21] Bekri Y. El., EdraouiM., Mouline J., & BassouA. (2023). Cyclic coupled fixed point via interpolative Kannan type contractions, *Mathematical Statistician and Engineering Applications*, **72(2)**: Paper no. 24.
- [22] Gaba Y.U. & Karapinar E. (2019). A new approach to the interpolative contractions, *Axioms* **8**: Paper no. 110.
- [23] Karapinar, E. Fulga, A., & Roldan Lopez de Hierro A.F. (2021). Fixed point theory in The setting of $(\alpha, \beta, \phi, \varphi)$ interpolative contractions, *Adv. Differential Equations* **2021**: 339.
- [24] Karapinar E., Fulga, A., & Yesilkaya, S.S. (2021). New results on Perov- Interpolative contractions of Suzuki type mappings, *J. Funct. Spaces*, Art. ID 9587604.
- [25] Khan, M.S., Singh, Y.M., & Karapinar E. (2021). On the interpolative (ϕ, φ) -type Z-contraction, *UPB Sci. Bull. Ser. A*. **83**:25-38.
- [26] Safeer K., & Ali R.(2023). Interpolative contractive results for m -metric spaces, *Advances in the Theory of Nonlinear Analysis and its Applications*, **7(2)**: 336-347.
- [27] Silkaya, Ye, S.S., Aydin C. & Aslan Y. (2020). A study on some multi-valued interpolative contractions, *Communications in Advanced Mathematical Sciences*. **3 (4)**: 208- 217.

□□



Nepal Journal of Mathematical Sciences (NJMS)

ISSN: 2738-9928 (online), 2738-9812 (print)

Vol. 5, No. 1, 2024 (February): 15-28

DOI: <https://doi.org/10.3126/njmathsci.v5i1.76443>

©School of Mathematical Sciences,

Tribhuvan University, Kathmandu, Nepal

Research Article

Received Date: December 12, 2024

Accepted Date: February 22, 2025

Published Date: February 28, 2025

Security of E-health Image in Cloud Environment Using Hybridization of DNA Cryptography: Systematic Literature Review

Madhav Dhakal^{1*} & Subarna Shakya²

¹Central Department of Computer Science and Information Technology, Tribhuvan University, Nepal

²Department of Electronics and Computer Engineering, Institute of Engineering, Pulchowk Campus

Tribhuvan University, Kathmandu, Nepal

Corresponding Author: * madhav.dhakal@mu.edu.np

Abstract: *This study focuses on addressing the critical issue of maintaining the confidentiality of valuable and confidential e-health records during transmission through cloud-based environments. It specifically investigates the hybridization of DNA-based computing with other encryption techniques. A systematic literature review was performed using the concept of the PRISMA framework. In this review, 12 kinds of literature related to the security of e-health images are selected from an initial pool of 1117 literatures from databases such as Science Direct, Springer Link, and Google Scholar. The reviewed studies were examined based on key security criteria, including resistance to statistical, differential, and exhaustive attacks, as well as randomness of pixels in images through entropy analysis. The findings indicate that the integration of DNA cryptography with chaotic maps offers a highly effective solution for enhancing data security during transmission. This hybrid encryption approach meets the minimum security requirements across multiple evaluated parameters, providing robust protection for sensitive e-health image data.*

Keywords: DNA Cryptography, Chaotic map, Cloud environment, e-Health, Data security

1. Introduction

Cloud computing is a mechanism for storing, accessing, and manipulating data over the internet, It has become an integral part of e-Health, e-Learning, e-Governance. The objective of cloud computing is to provide quick, simple data storage and computing service. In today's technology-driven world, all institutions have started to transmit and store confidential data in cloud environments. Maintaining the confidentiality of this data is the most crucial and significant task. To achieve this, it is mandatory to adopt any reliable and trustworthy security technique that ensure the protection of users data. Several cryptographic approaches like symmetric, asymmetric, biometric, quantum,

block chain , and other non-cryptographic approaches, including server-side application security, hardware-level security, operating system security have been implemented in cloud computing.

Most of the healthcare organizations adopt cloud computing services to enhance service quality. To address this, they are shifting their operations from a traditional manner to an online service. They began storing data in cloud databases and provide the e-health services, such as telemedicine or smart health care. Cloud databases improve efficiency, but they also offer a significant impact and challenge to the security of shared data. Thus, data stored in the cloud has to be secured in a proper and systematic way.

In e-health, all health-related documents are stored on highly capable storage devices, such as cloud computers or local drives and all confidential details of patients are transmitted to remote areas with the public unsecured network like internet. Such valuable data is then used by the medical entities, just as doctors use those records at every new checkup time and also deliver them to the patient through email whenever necessary. Sukumaran and Mohammed[21] have considered an authentic health record to be the most valuable document in a patient's life. If tiny changes are made unexpectedly, it affects the whole treatment process in the future, which affects not only the health of the patient but also the reputation of the hospital and medical team. For better, faster, and more secure transmission of health-related documents, e-health data must be kept secure and confidential way, and a confidential mechanism for storage is mandatory. Banu et al.[7] have studied that in image data security, large volume of data, data redundancy, and highly correlated adjacent pixel intensities, traditional cryptosystems like AES, RSA are not applicable. Therefore, different image encryption algorithms, including integration of the chaotic system with DNA computing and cellular automata, are used.

In this review, we focus on the security of data using DNA based concepts, either as a standalone method or integration with other innovative techniques. DNA cryptography uses DNA as an information carrier to solve complex problems, including the clique problem of a graph, the directed Hamilton problem of seven vertices, the Turing problem, and the NP-complete problem. In DNA-based cryptography information is secured using the four nucleotides, i.e., Adenine (A), Cytosine (C), Guanine (G), and Thymine (T). Here, Adenine is complementary to Thymine and Cytosine is complementary to Guanine.

The structure of this paper is outlined as follows: Section 2 reviews related studies; Section 3 discusses the motivation and limitations of this study; Section 4 outlines the materials and methods; Section 5 provides a security analysis and its parameters; Section 6 presents results and discussion; and section 7 summarizes the conclusion and future directions.

1.1. Research Questions

The research questions of the study are set as:

- What are the existing hybridization techniques that combine DNA cryptography with other encryption techniques for securing e-health images in cloud environments?
- How effective are hybrid DNA cryptography techniques in mitigating brute force attacks on e-health images transmitted in cloud environments?

1.2.Objectives of the Study

To accomplish the research questions, research objectives of the study are set as:

- To evaluate the effectiveness of hybrid DNA cryptography techniques in mitigating brute force attacks on e-health images transmitted in cloud environment.
- To identify the real-world applications of hybrid DNA cryptography for securing e-health images in cloud environment.
- To evaluate the outcomes of hybrid DNA cryptography in terms of security and usability for securing e-health images.

2. Related Work

The transmission of data using cloud-based technology is increasing everywhere and the risk of data breaches and alternations caused by unauthorized users is also growing at the same rate. Several researchers have published works to address the security of data in cloud environments using the concept of DNA computing and its integration with other innovative techniques. Among them, an overview of some works is listed as follows:

Can et al.[8]have explored innovative cryptographic methods inspired by genetic science base encryption technique to strengthen cloud data security. These methods show promise for enhancing data security but present challenges related to computational complexity and practical implementation within real-time cloud applications. The paper underlines the potential of genetics-based cryptographic techniques to address specific cloud security but also points out gaps in scalability and adaptability, which could hinder widespread adoption. Thus, while genetic cryptography introduces innovative possibilities, further research is needed to resolve these limitations and fully harness its capabilities in large-scale cloud applications.

Sukumaran and Mohammed[21] have proposed the implementation of the DNA-based authentication technique for the awareness of the health record and remedies of childbirth and about pregnant women through the message, voice, and flash alter. The main concept behind this technique is to link the Electronic Health Records (HER) and DNA, which ensure the usability and confidentiality of electronic data and help minimize maternal and infant mortality rates in India.

Le [15] has studied the CS-E2E protocol, a DNA-based authentication approach designed for healthcare services in the Internet of Living Things (IoLT). This protocol enables mutual authentication between patients and establishes a secure, shared key for private communication, bolstered by multiple security measures such as Single Sign-ON (SC-SSO), Elliptic Curve Cryptography (ECC), and bio-hashing. Security analyses demonstrate that CS-E2E is resistant to a range of attacks and maintains cost-efficiency in terms of computational and communicational overhead. However, while the study provides a promising framework for patient authentication, it could benefit from further examination of scalability under high network loads, as well as potential vulnerabilities when integrated with broader IoLT applications.

Joseph and Mohan[14] introduced an innovative algorithm aimed at ensuring secure data sharing in cloud environments by integrating the Grey Wolf Optimization Algorithm (GWOA) with DNA cryptography. The algorithm begins by transforming the data into DNA sequences, followed by the generation of cryptographic keys using GWOA. During the encryption phase, XOR and complementation are applied to the DNA sequences to secure

the data. For decryption, reverse operations are carried. The results from various tests indicate that the proposed concept is highly effective and secure during the transmission of data through cloud-based systems.

In the face of escalating cyber threats to electronic health records (EHRs), the research by Banu et al. [7] introduced a robust encryption framework for medical images that leverages DNA subsequences, SHA-256 hashing, and the Hyper Chaotic Multi-Attractors Chen System (HCMACS). The integration of HCMACS generates pseudorandom keys, enhancing the resilience and unpredictability of the encryption. The approach achieves the CIA triad, and its performance has been validated against statistical, differential, and chosen-plaintext attacks, affirming the model's robustness. A key advantage lies in its sensitivity to initial conditions, where secret keys are tightly linked to the hash of the original image, adding an extra layer of security. While the model shows considerable strength in protecting EHR data, its reliance on computationally intensive operations, such as DNA-based encoding and hyper-chaotic mapping, may raise efficiency concerns for real-time applications.

To encrypt the medical images, Dagadu et al. [9] recommended a hybrid chaotic and DNA technology. The cipher image is created by performing a row-by-row diffusion process utilizing the DNA XOR algebraic operation between the plain image matrix and the two chaotic key matrices in an alternating pattern. The DNA encoding and decoding rules are chosen for each row using the logistic map. Experimental findings from statistical, differential, and key studies show that the suggested system is reliable and offers defense against a variety of attacks.

Akkasaligar and Biradar[4] suggested DNA cryptography and the dual hyperchaotic map for maintaining the confidentiality and sensitivity of selected digital images in the medical area. Only a few images are used here due to the large size and longer calculation time of digital images. Confusion and Diffusion mechanisms are used on certain image pixels during the encryption of specific images using this hybrid technology, and then DNA encoding rules are used. This approach requires less computing time and is highly effective for securing e-health images.

In 2021, Elamir et al. [10] proposed a three-stage technique for hiding medical images, where first the information is hidden using the least square bit of pixel, and the resultant image is compressed with the combination of six chaotic maps, namely Chebyshev, Gauss, Logistic, Tent, and Piecewise maps, and then into DNA encoding format. In the DNA encoding technique, e-health images are stored through DNA molecules, so the size of the image is reduced and the data transmission rate is increased.

To maintain healthcare security between patient and doctor, Naing et al. [13] in 2023 proposed a symmetric key encryption algorithm called Key Encryption Decryption (KED) using modulo 92, aimed at protecting Patient Health Information (PHI). This approach combines AES S-box transformations with DNA cryptography for a more robust security framework. Especially, it is designed to resist cryptographic attacks like differential and linear cryptanalysis.

Researchers Qiqieh et al. [19] proposed a DNA-based Cryptographic Security Framework (DNA-CSS) with the concept of Diffie-Hellman key exchange and the Feistel structure of cryptography to improve the health record in cloud environments. This study combines a strong key agreement protocol and encryption algorithm with a new wrapping technique for encryption and decryption techniques. However, the absence of a thorough comparison with other cutting-edge encryption frameworks for medical records and the requirement for practical testing.

3. Motivations and Limitations of the Study

This study examines data security in the e-health sector, focusing specifically on approaches that incorporate the hybridization of DNA-based cryptography with other established security standards. Given the increasing importance of protecting sensitive health information, this review aims to explore how DNA cryptography, a relatively novel approach inspired by the structure and encoding properties of biological DNA, can be integrated with conventional techniques to enhance data security in e-health applications.

A notable limitation of this study is that, despite availability of various data security techniques, the selected literature primarily emphasizes DNA-based cryptography in medical sectors. This restricted focus means that other well-established data security methods used in the e-health sector are not covered in detail, which may limit the generalizability of findings. As a result, this review highlights only a specific subset of security solutions within a broader field.

4. Materials and Methods

This review of the literature covers the data source and search strategy, study selection, & inclusion-exclusion criteria, data extraction mechanism, analysis & publication, and results.

Information source and Search strategy

Preferred Reporting Items for Systematic Review and Meta-Analysis (PRISMA) guideline by Page et al.[18] are followed for this review. At the final stage of these phases, it is assumed that the review process is free of biases and that the final outcome will maintain the consistency and accuracy of the review. Several scientific papers were accumulated from the international standard digital bibliographic databases like Science Direct, Springer Link, and search engine Google Scholar, which are the primary sources for finding the literature related to data security in Images of e-health using the hybrid concepts of DNA cryptography. Searching for data was done from 2020 to December 14, 2023. A total of 1117 pieces of literature are downloaded, and out of them, 672 are from Springer Link, 247 from Science Direct, and 198 from Google Scholar. To find the literature related to our review, "Data security", "DNA cryptography", "Medical Image Encryption", "Cloud Data security", "Chaotic Map" keywords are used with the combination of "AND, OR," and "NOT" operators to narrow or broaden the search. We also searched the literature on the basis of alternative words for the included keywords. Combination of keyword and operator is randomly interchanged until and unless our required literature is not found. Retrieved literature from databases was found via their search engine. In Springer Link and Google Scholar, results were retrieved using the provided export function in CSV format, but in Science Direct, datasets were downloaded in BibTex format, and further with the JebRef tool, they were converted into CSV format, after that, all datasets were compiled in Microsoft Excel with the same file but different worksheets.

Study Selection and Inclusion Exclusion Criteria

Among the various reference management systems, the current study uses Zotero to manage the literature searched from the above databases and search engines. It is open-source software that can be downloaded easily and freely. First, all selected articles are exported into Zotero either by entering their ISDNs, DOIs, or any unique number, or by linking the downloaded file or storing a copy of the file. It merges the results and eliminates any duplication, if any are found. In this systematic review, inclusion/ exclusion, and restriction criteria are listed as: Those literatures are included if 1) they are related to cloud data security, 2) they are related to the images of e-health or with other synonyms 3) original paper, peer review article, conference proceeding paper 4) Studies on hybrid cryptography with DNA cryptography or image encryption 5) written in English and from the field of computer science & Information Technology 6) published between 2020 to December 14, 2023. Studies are excluded if they are: 1) duplicate research

papers; or 2) not related to the security of the e-health image. 3) Thesis report 4) non peer-reviewed article; 5) having inadequate information.

Using the PRISMA Framework, 1031 literatures were eliminated by screening titles, abstracts, and published years and the remaining 86 literatures were thoroughly reviewed. 71 of the 86 items were not matched with our review topic, so these are also excluded from our review, and out of the remaining 15 articles, 1 is not in English, 1 is a thesis document, and another 1 does not contain full information. The current systematic review and analysis study employed and included 13 articles. Finally, all selected literature's evaluation factors were examined, and their results were summarized.

Data Extraction

All reviewers studied the inclusion literature for the extraction of data in a systematic way independently, and all of them came together to verify if any uncommon views or confusion were observed between them. To extract the result, each reviewer, contributes equally.

Quality Assessment

During the review process, a critical component of a systematic review of the literature is quality assessment. In this study, each researcher carefully examined and ranked the standard of each abstract independently to assess the quality and maintain the similarities, standard, and unbiased judgment and purification of each selected article. To maintain the quality of the review, only original, peer-reviewed publications and conference proceedings were used. After analyzing and evaluating all relevant articles, all authors evaluate the quality of the research. The numbers of downloaded and reviewed literatures in our study are presented in Fig-1, and the overall steps of the study are given in Fig-2.

Data Synthesis

Synthesis of data is carried out to systematize and aggregate the results of the study. And determine whether the obtained result supports the objective to address the answer of the research question or not.

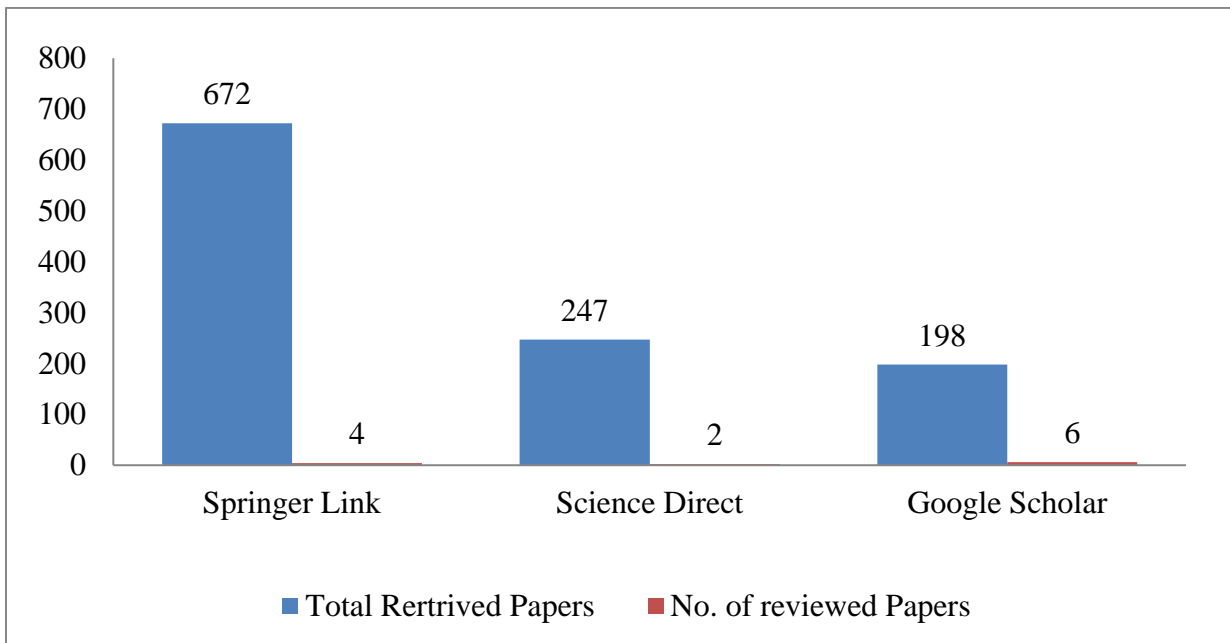


Fig-1: Number of downloaded and selected papers for review

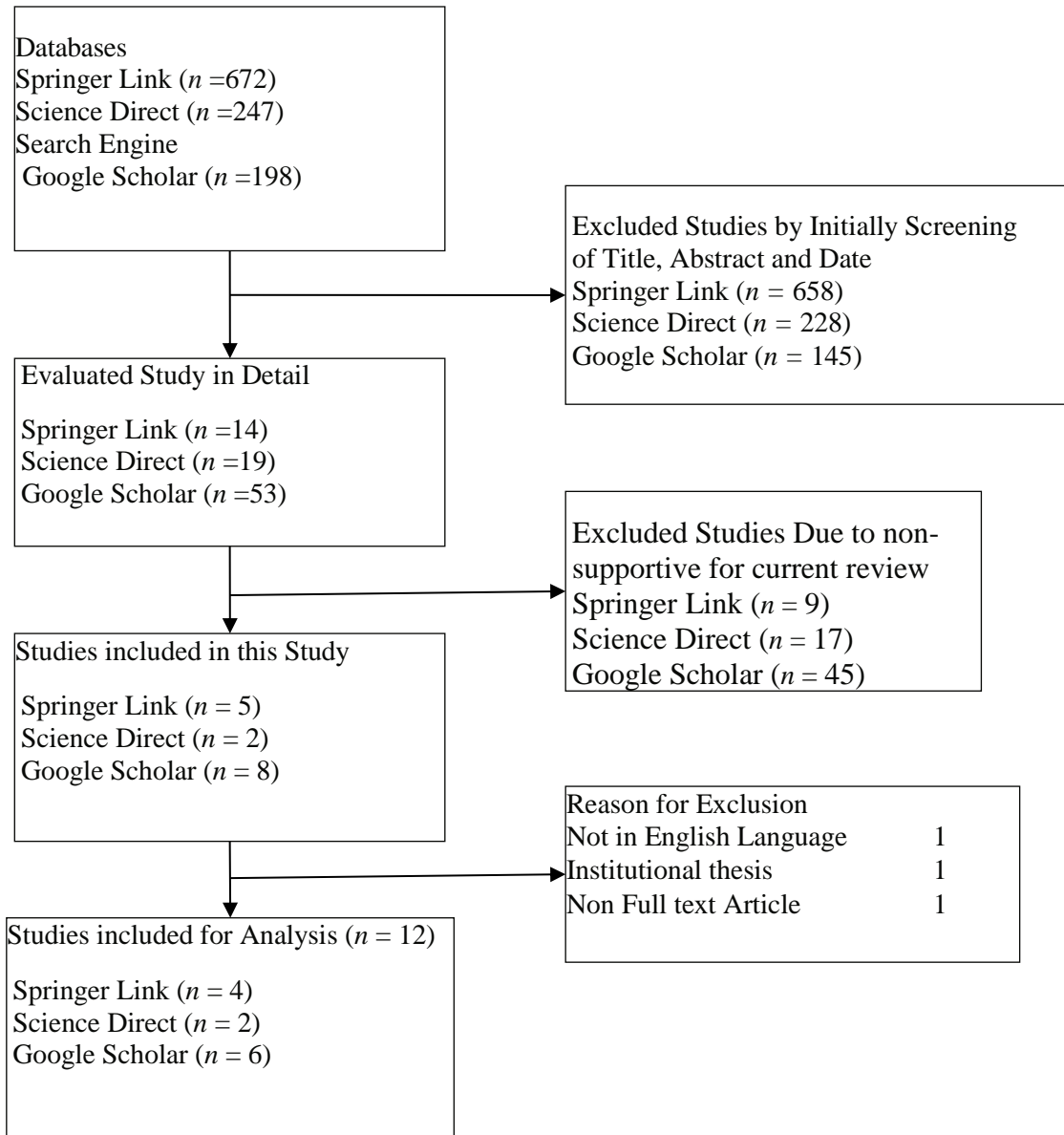


Fig-2: PRISMA framework for selection of literatures

5. Security Analysis Parameters

All the selected reviewed articles focus on securing medical images by leveraging the hybrid characteristics of DNA cryptography. Result obtained from the secured encrypted image is test over the various parameters including (a) Histogram analysis (b) Correlation analysis (c) Encryption/Decryption time (d)Entropy (e)Unified Average Changing Intensity(UACI)(f) Number of Changing Pixel Rate(NPCR) (g)Mean Square Error(MSE) (h) Peak Signal to Noise Ratio(PSNR) and(i) Structure Similarity Index Measurement(SSIM).

- a. **Histogram Analysis:** Histogram analysis is carried out to analyze the pixel distributions in the image. If the distribution of pixel intensities in encrypted image is uniform, the encryption technique is considered secure. Otherwise, an unauthorized person may access the valuable information from the image .
- b. **Correlation Analysis:** In image data security, correlation analysis is carried out to determine the quality of the ciphertext image. Correlation analysis is carried out between two adjacent pixels of an image. In the plaintext image, the correlation between neighboring pixels is high (near about 1), i.e., there is, more redundancy, but in a better cryptosystem, the correlation is low (near about 0), which means, that the encrypting algorithm is better. Correlation coefficients are calculated using a formula.

$$r_{x,y} = \frac{\text{cov}(x,y)}{\sqrt{D(x)} \sqrt{D(y)}} \quad (1)$$

$$\text{cov}(x, y) = E\{(x - E(x))(y - E(y))\} \quad (2)$$

$$E(x) = \frac{1}{N} \sum_{i=1}^N x_i \quad (3)$$

$$D(x) = \frac{1}{N} \sum_{i=1}^N (x_i - E(x))^2 \quad (4)$$

Where x and y are gray scale values of neighboring pixels in the original image and ciphered image with correlation coefficient $r_{x,y}$.

- c. **Encryption/Decryption Time:** It is the total time taken for the encryption of the original image and the return to the original image from the cipher image.
- d. **Entropy:** Entropy measures the degree of randomness and disorder in data. For an enciphered image of 256 grayscale levels, entropy is 8. Thus, the randomized image has entropy near about 8. Entropy of image is calculated as:

$$H(x) = - \sum_{i=0}^{255} p(x_i) \log p(x_i) \quad (5)$$

Where, $x_i \in p(x)_i$ is the probability of occurrence.

- e. **Unified Average Changing Intensity (UACI):** UACI represents the average change in intensity level in two ciphered images. It is calculated by the equation:

$$\text{UACI} = \sum_{i,j} \frac{|C_1(i,j) - C_2(i,j)|}{255 * M * N} * 100\% \quad (6)$$

Where C_1 is the encrypted form of original image O_1 and C_2 is the encrypted image of O_2 , where O_2 is obtained by single pixel change in O_1

- f. **Number of Changing Pixel Rate (NPCR):** NPCR calculates the number of changing pixels in both the cipher image and the same position. NPCR can be determined as:

$$\text{NPCR} = \frac{\sum_{i,j} D(i,j)}{M * N} * 100\% \quad (7)$$

$$D(i, j) = \begin{cases} 0 & C_1(i, j) = C_2(i, j) \\ 1 & \text{Otherwise} \end{cases}$$

If the value of NPCR is small, then it means that there is a small variation between two cipher images. Therefore, the NPCR value must be near 100%.

- g. **Mean Square Error (MSE):** MSE calculates the differences between two images. Which is given by the equation as:

$$MSE = \frac{\sum_{i=1}^M \sum_{j=1}^N [I_1(i,j) - I_2(i,j)]^2}{M \times N} \quad (8)$$

Where I_1 and I_2 are the pixel values of the original and encrypted images, respectively, and (i, j) is the pixel location. M and N are the dimensions of images. If the resultant value obtained from the above equation is large, it means the encryption algorithm is better.

- h. **Peak Signal to Noise Ratio (PSNR):** PSNR value is used to check whether noise affects the quality of an image. PSNR is inversely proportional to the MSE of the image. It is calculated as

$$PSNR = 20 * \log_{10} \left(\frac{255}{\sqrt{MSE}} \right) \text{dB} \quad (9)$$

- i. **Structure Similarity Index Measurement (SSIM):** To determine the degree of similarities in plaintext image and deciphered image the value of SSIM is use. It is calculated from the equation as:

$$SSIM = \frac{(2\mu_I\mu_D + C_1) + (2\sigma_{ID} + C_2)}{(\mu_I^2 + \mu_D^2 + C_1)(\sigma_I^2 + \sigma_D^2 + C_2)} \quad (10)$$

Where C_1, C_2 are constants, (μ_I, μ_D) is the average of deciphered (D) and input (I) image. Similarly, (σ_I^2, σ_D^2) is the variance of I, D and σ_{ID} is covariance between D and I .

6. Result and Discussion

The key space requires to encode the original message to prevent from the exhaustive attack is listed in Table 1. Here, results from the reviews are placed in structured ways in tabular form and the reviewed literature demonstrates a key space larger than 2^{100} , indicating that each technique provides robust security against brute-force attacks in a cloud environment. This substantial key space ensures that the adopted methods effectively safeguard data by making brute-force attempts computationally infeasible. In some of these selected literatures, key space analysis is not listed but these researches utilize the concept of chaotic system and it demonstrate the initial value sensitivity, it means, when unauthorized person try to access the information with tiny modification in secured key then the image is not decrypted properly. This characteristic shows the robustness in image data security. Trends in publications of literature with their applications, proposed method, and result are expressed as Table 2 and various metrics related with the literatures are listed in Table 3.

These tabulated results addressed the research questions and associated objectives of the present review of e-health image data security in cloud environments based on various security analyses, offering a clear perspective on the evidence gathered and the thematic trends observed.

Table 1. Key Length in Selected Study

References	Key length
Aashiq Banu and Amirtharajan [1]	2^{680}
Adithya and Santhi [2]	2^{128}
Ahuja et al.[3]	2^{448}
Akkasaligar and Biradar [4]	2^{366}
Akkasaligar and Biradar [5]	2^{399}
Alqazzaz et al.[6]
Elamir et al. [10]
Elamir et al. [11]
Ettiyan and Geetha [12]
Liu et al.[16]	2^{704}
Nezhad et al. [17]
Sarosh et al. [20]

Table 2. Summary of Reviewed Article

Ref.	Encryption Technique	Application	Result
Ahuja et al.[3]	DNA computing with Arnold Map	Generate more secure medical images than the lower-dimension chaotic map.	Proposed method provides better protection of the image and visual data in the field of biometric and normal grayscale images.
Akkasaligar and Biradar[5]	DNA computing with dual hyper-chaotic map	Reduce the computation time of image.	Take less computation time. Diffusion and confusion is conducted only for the selected image.
Akkasaligar and Biradar[4]	DNA computing with 4D Lornez chaotic map	Use Discrete Haar Wavelet for lossless compression of images.	Compressed image was changed into four different sub image, which was shuffled using 4D chaotic map,
Adithya and Santhi[2]	DNA computing with chaos map, Knight's Travel map	Applicable for smart healthcare including telemedicine, e-health.	Reduces computing time while offering adequate security. On selected pixels of medical images, the proposed DMIES cryptographic system applies the chaos intertwining logistic map diffusion and confusion process.
Alqazzaz et al.[6]	DNA computing with hyperchaotic RKF-45	Application in image data security in e-health system.	Ciphertexts' efficiency and unpredictability were increased by using DNA addition and subtraction operations.

Liu et al.[16]	DNA computing with SHA-512	Encrypt medical image using the integration of chaotic properties and Sin-Arcsin-Arnold Multi Dynamic random nonadjacent Coupled Map Lattice (SAMCML).	The SAMCML technique secures multi-images with various algorithms. Security analysis results close to optimal values with strong robustness.
Ettiyan and Geetha [12]	Hybrid chaotic DNA and AES encryption	This study focuses on developing a more secure system to prevent security breaches in IoT.	Combining a 3D chaotic map with DNA encoding for enhanced IoT security in medical data transmission. Experimental evaluations demonstrate the system's strong performance and robustness.
Nezhad et al. [17]	DNA sequencing and Tent Chaotic system	Secure fingerprint images during transmission.	Encrypt the fingerprint images using chaotic mapping and DNA sequencing with XOR operations.
Elamir et al. [11]	RSA with DNA Cryptography	To block the unauthorized access from the IoT devices in network. It reconstructs the medical image with high quality.	Enhance image data security in cloud computing, a hybrid approach of RSA with DNA based cryptography.
Sarosh et al. [20]	PWLCM and DNA Cryptography	To maintain the confidentiality of medical images during transmission from IOT devices using the concept of DNA-3D chaos and PWLCM system.	The approach stated in the research leads to lossless medical data recovery. The image obtained through the Map, maintain the security by diffusion the pixel of that image.
Elamir et al. [10]	DNA encoding and Least Significant Bit	Hiding the confidential information of patient's in medical with Least Significant Bit.	Six stages generated key for image compression : Chebysev, Gauss, Henon.Logistic,Tent , and Piecewise maps of chaotic map.
Aashiq Banu and Amirtharajan [1]	DNA and Chaotic Fused approach	Propose a new way of scrambling and then DNA method was used to encrypt the digital image,	Strong resistance to statistical attack, exhaustive attack and others parameters. This study highlights hybrid chaos-DNA based cryptosystem.

Table 3. Security Analysis of Review Article

Ref.	System	Enc / Dec Time	Hist.	Entropy	Cor.	PSNR/MS E	NPCR/UA CI (%)
Ahuja et al.[3]	Uniform	7.99	Negative	$\infty/0$	99.95/32.53
Akkasaligar and Biradar[4]	Intel Core i7,7 th Generation	14/23	Uniform	7.99	99.72/37.68
Akkasaligar and Biradar[5]	Intel Core i7, RAM:8GB, CPU: 2.70GHz	0.236/0.248	Uniform	7.8446	0.00154/0.9946	5.72 / 739.13	99.68/33.55
Adithya and Santhi[2]	Intel Core i5, RAM:4GB CPU: 2.7GHz	0.233/0.243	Uniform	7.9975	7.91/12077.1 ²	99.789/33
Alqazzaz et al.[6]	Intel Core i7-4910MQ, CPU: 2.90GHz , RAM: 16GB	Uniform	7.99	≈ 0	99.603/33.32
Liu et al.[16]	Uniform	7.9994	≈ 0	99/33
Ettiyan and Geetha [12]	AWS cloud server, 1,4GHz processor, MICOT BOARDS
Nezhad et al. [17]	Uniform	7.98	99.60/33.46
Elamir et al. [11]	Dell Core i7, 8 GHz RAM	31.329/18.472	Uniform	0.85746	41.439/1.39 e-04	X/32.68
Samiullah et al.[20]	Window 7,core I3, RAM: 4GB	22.43/23.12	Uniform	7.99	Near 0	$\infty/0$	99.62/33.40
Elamir et al. [10]	Intel i7, RAM: 8 GB	Depend upon Image	Uniform	< 8	Near 0	> 11.6 /> 10000	$\approx 99 / \approx 0$
AashiqBanu and Amirtharajan [1]	Window 10, Xeon(R) E3-1220 v6 at 3GHz , 32 GB HD	Uniform	7.99	Near 0	$\infty/0$	99.6 / 33.4

7. Conclusion and Future Work

Maintaining the confidentiality of e-health images is one of the most pressing and intriguing challenges in the current landscape. This paper presents a systematic review of techniques for securing medical images, focusing on a hybrid approach that combines DNA cryptography with other methods to protect data during transmission. Twelve articles from various databases and search engines are reviewed based on different security metrics. All selected studies address the security of medical images through the hybrid approach of DNA cryptography. Some of these literatures integrate the DNA computing technique with chaotic system and some other with RSA, and AES. From analyzing key space and other security parameters it is evident that the combination of DNA cryptography with other techniques provides a comparable level of confidentiality for medical images across multiple security parameters. DNA encoding techniques are frequently used alongside chaotic maps and other security measures, with results showing that this combined approach is increasingly effective for image security.

Overall, the reviewed security measures for safeguarding medical data through DNA-based techniques are satisfactory. Looking ahead, this review proposes the development of a new model incorporating DNA based computing and other standard data security measures to further enhance data confidentiality and integrity.

References

- [1] Aashiq Banu, S. & Amirtharajan, R. (2020). Tri-level scrambling and enhanced diffusion for DICOM image cipher DNA and chaotic fused approach. *Multimedia Tools and Applications.*, **79(39)**: 28807-28824.
- [2] Adithya, B. & Santhi, G. (2022). A DNA Sequencing Medical Image Encryption System (DMIES) Using Chaos Map and Knight's Travel Map. *International Journal of Reliable and Quality E-Healthcare (IJRQEH).*, **11(4)**: 1-22.
- [3] Ahuja, B., Doriya, R., Salunke, S., Hashmi, M. F. & Gupta, A. (2023). Advanced 5D logistic and DNA encoding for medical images. *The Imaging Science Journal.*, **71(2)**: 142-160.
- [4] Akkasaligar, P.T. & S. Biradar, S. (2020). Medical Image Compression and Encryption using Chaos based DNA Cryptography, *IEEE Bangalore Humanitarian Technology Conference.*, 1–5.
- [5] Akkasaligar, P. T. & Biradar, S. (2020). Selective medical image encryption using DNA cryptography. *Information Security Journal: A Global Perspective.*, **29(2)**: 91-101.
- [6] Alqazzaz, S. F., Elsharawy, G. A. & Eid, H. F. (2022). Robust 4-D Hyperchaotic DNA Framework for Medical Image Encryption. *International Journal of Computer Network & Information Security.*, **14(2)**: 67-76.
- [7] Banu, S. A., Al-Alawi, A. I., Padmaa, M., Priya, P. S., Thanikaiselvan, V. & Amirtharajan, R. (2024). Healthcare with data care—a triangular DNA security. *Multimedia Tools and Applications.*, **83(7)**: 21153-21170.

- [8] Can, O., Thabit, F., Aljahdali, A. O., Al-Homdy, S. & Alkhzaimi, H. A. (2023). A comprehensive literature of genetics cryptographic algorithms for data security in cloud computing. *Cybernetics and Systems.*, 1-35.
- [9] Dagadu, J. C., Li, J. P. & Aboagye, E. O. (2019). Medical image encryption based on hybrid chaotic DNA diffusion. *Wireless Personal Communications*, **108**: 591-612.
- [10] Elamir, M. M., Al-atabany, W. I. & Mabrouk, M. S. (2021). Hybrid image encryption scheme for secure E-health systems. *Network Modeling Analysis in Health Informatics and Bioinformatics.*, **10(1)**:35.
- [11] Elamir, M. M., Mabrouk, M. S. & marzouk, S. Y. (2022). Secure framework for IoT technology based on RSA and DNA cryptography. *Egyptian Journal of Medical Human Genetics*, **23(1)**: 116.
- [12] Ettiyan, R. & Geetha, V. (2023). A hybrid logistic DNA-based encryption system for securing the Internet of Things patient monitoring systems. *Healthcare Analytics.*,**3**: 100149.
- [13] Naing,H.H., Aye,Z.M. & Naing,S.K.(2023). E-Health System Based KED and DNA Cryptosystem, *IEEE Conference on Computer Applications.*, 169-173.
- [14] Joseph, M. & Mohan, G. (2022). A Novel Algorithm for secured data sharing in cloud using GWOA-DNA cryptography. *International Journal of Computer Networks and Applications.*, **9(1)**: 114-124.
- [15] Le, T. V. (2023). Cross-server end-to-end patient key agreement protocol for DNA-based U-healthcare in the internet of living things. *Mathematics.*, **11(7)**: 1638.
- [16] Liu, H., Teng, L., Zhang, Y., Si, R. & Liu, P. (2024). Mutil-medical image encryption by a new spatiotemporal chaos model and DNA new computing for information security. *Expert Systems with Applications.*, **235**: 121090.
- [17] Nezhad, S. Y. D., Safdarian, N. & Zadeh, S. A. H. (2020). New method for fingerprint images encryption using DNA sequence and chaotic tent map. *Optik*, **224**: 165661.
- [18] Page, M. J., McKenzie, J. E., Bossuyt, P. M., Boutron, I., Hoffmann, T. C., Mulrow, C. D. & Moher, D. (2021). The PRISMA 2020 statement: an updated guideline for reporting systematic reviews. *bmj*, 372.
- [19] Qiqieh, I., Alzubi, J. & Alzubi, O. (2025). DNA cryptography based security framework for health-cloud data. *Computing.*,**107(1)**: 35.
- [20] Sarosh, P., Parah, S. A. & Bhat, G. M. (2022). An efficient image encryption scheme for healthcare applications. *Multimedia Tools and Applications.*, **81(5)**: 7253-7270.
- [21] Sukumaran, S. C. & Misbahuddin, M. (2018). DNA Cryptography for Secure Data Storage in Cloud. *Int. J. Netw. Secur.*, **20(3)**: 447-454.



A Short Note in Quantum Continuity Equation

Bishnu Hari Subedi^{1*} & Tara Bahadur Rana²

¹Central Department of Mathematics, Tribhuvan University, Kirtipur, Kathmandu, Nepal

²St. Xavier's College, Maitighar, Kathmandu, Nepal

Corresponding Author: *subedi.abs@gmail.com

Abstract: In this article, we present a view that the interpretation of quantum mechanics lacks unanimous approval among physicists. To show its inadequacy, we describe the well-known measurement problem and discuss two solutions: an orthodox solution and hidden variables.

We provide a brief overview of Bohmian mechanics. We then derive the continuity equation for quantum mechanics and show that a realist interpretation of the quantum probability current \vec{j} leads to the guiding equation for Bohmian mechanics.

Keywords: Quantum continuity equation, Quantum probability current, Guiding equation.

1. Introduction

Before the advent of quantum mechanics, the basic understanding of natural phenomena came from classical mechanics; however, after the development of quantum mechanics, it superseded classical mechanics. We know quantum mechanics is more fundamental than classical mechanics, as classical mechanics emerges from quantum mechanics under appropriate limits. Historically, there were two independent formulations of quantum mechanics: *wave mechanics* (Schrödinger) and *matrix mechanics* (Heisenberg, Born, Jordan). Both founding fathers (Schrödinger and Heisenberg) thought that their version of the formulation was superior [7, 12].

Any scientific theory consists of two important parts: *formalism* and *interpretation*. Formalism deals with the mathematical aspect of the theory, which is essential in giving new predictions that can be tested. The interpretation provides the answers of the question of what exists at the fundamental level of reality [10]. The ontology of Newtonian mechanics is a particle. However, when one asks, “What is the ontology of quantum mechanics?” One cannot provide a unanimous answer agreed by most physicists and philosophers. Despite robust mathematical formalism, quantum mechanics has multiple interpretations that answer the question of “what exists?” It is a question whose answer is murky and clouded by various interpretations and the fancy structure they demand.

2. The Measurement Problem

Quantum mechanics postulates that the state vector in Hilbert space represents the state of a system that evolves from the Schrödinger equation, or in the light of matrix mechanics the evolution is described by a unitary operator. However, we get a conflict between what the dynamics predicts and what we observe; this is what we deem as “the measurement problem”. We will present the problem following the approach given in [9] for a formal treatment [4].

Let’s say we want to measure the electron spin. For this task, we have a sophisticated device that measures the spin and let S be the unitary operator associated with the physical observable spin.

If the electron is in $|\uparrow\rangle$ the device measures it as $|\uparrow\rangle$, similarly if it is in $|\downarrow\rangle$ then the device measures it as $|\downarrow\rangle$. Now instead of $|\uparrow\rangle$ or $|\downarrow\rangle$, we have $|\psi\rangle$ which is the superposition of both $|\uparrow\rangle$ and $|\downarrow\rangle$,

$$|\psi\rangle = \frac{1}{\sqrt{2}}(|\uparrow\rangle + |\downarrow\rangle).$$

Now we apply the spin operator,

$$S|\psi\rangle = \frac{1}{\sqrt{2}}(S|\uparrow\rangle + S|\downarrow\rangle),$$

it then follows that the system should evolve in the following way:

$$\frac{1}{\sqrt{2}}(S|\uparrow\rangle + S|\downarrow\rangle) \Rightarrow \frac{1}{\sqrt{2}}|\uparrow\rangle + \frac{1}{\sqrt{2}}|\downarrow\rangle$$

which is a superposition of two spin states. But we would never observe a superposition instead, we observe the following:

$$\text{either } S|\uparrow\rangle = |\uparrow\rangle \text{ (with frequency approximately } 1/2)$$

or

$$S|\downarrow\rangle = |\downarrow\rangle \text{ (with frequency approximately } 1/2).$$

The predictions made by the dynamics and our observation contradict one another. What we get by measuring an electron that is in superposition is, sometimes we get $|\uparrow\rangle$ and sometimes $|\downarrow\rangle$ the best we can do is get the probability of finding the electron in spin $|\uparrow\rangle$ or $|\downarrow\rangle$, which is given by Born’s rule.

3. Solutions

3.1 Orthodox Solution

One of the solutions to the measurement problem was given by Paul Dirac and John von Neumann, dubbed the orthodox solution [7, 8]. Neumann proposed that there are two kinds of processes happening in nature.

Process 1 is the process where the wave function collapses into a determinate value whose probability is given by the Born's rule; this is a stochastic, non-linear process.

Process 2. The wave function evolves deterministically according to the Schrödinger equation.

Also, by introducing the concept of measurement into our laws, we are making this theory about observers, which does not sound right to invoke complex organisms as observers as part of its most basic framework [3].

3.2 Hidden Variables

A different interpretation of quantum mechanics, called Bohmian mechanics or hidden variables, was formulated by David Bohm in his seminal papers [5, 6]. Bohmian claims that the wave function does not give a complete description of reality [11].

The wave function is not fundamental and serves only as a pragmatic tool. Bohmian mechanics posits that the particle, which has a definite position, is more fundamental than the wave function. This particle is guided by the wave function.

Bohm's theory solves the measurement by positing determinate particle position, which does not involve the idea of measurement or observer as the fundamental part of the framework [3]. Now, we will present the postulate of Bohmian mechanics as presented in [1].

3.2.1 The state description

The description of a Bohmian state for a particle is specified by (ψ, q) , where ψ is the wave function, and q is the actual position of the particle.

3.2.2 The dynamics

The Schrödinger equation gives the evolution of ψ :

$$i\hbar \frac{\partial \psi}{\partial t} = \hat{H}\psi$$

where i is the complex number, \hbar is reduced Planck constant, and \hat{H} is the Hamiltonian of the system. The evolution of the particle position is given by the guiding law (or equation of motion):

$$v = \frac{\nabla S}{m},$$

S is the phase of the wave function and m is the mass of the Bohmian particle.

3.2.3 The quantum equilibrium

The quantum equilibrium configuration probability distribution ρ for an ensemble of systems each having quantum state ψ is given by:

$$\rho = |\psi|^2. \tag{1}$$

4. Guiding Equation from Quantum Continuity Equation

The continuity equation in quantum mechanics is analogous to the continuity equation of electrodynamics and fluid mechanics. Let's take a single-particle system moving in one dimension in real potential V , then the Schrödinger equation is:

$$i\hbar \frac{\partial \psi}{\partial t} = -\frac{\hbar^2}{2m} \frac{\partial^2 \psi}{\partial x^2} + V(x, t)\psi, \tag{2}$$

and its complex conjugate is:

$$-i\hbar \frac{\partial \psi^*}{\partial t} = -\frac{\hbar^2}{2m} \frac{\partial^2 \psi^*}{\partial x^2} + V(x, t)\psi^*. \quad (3)$$

Multiplying equation (2) by ψ^* , multiplying equation (3) by ψ , and subtracting the second from the first we get

$$\frac{\partial |\psi|^2}{\partial t} = -\frac{\partial}{\partial x} \left[\frac{i\hbar}{2m} \left(\psi \frac{\partial \psi^*}{\partial x} - \psi^* \frac{\partial \psi}{\partial x} \right) \right]. \quad (4)$$

This takes the form of a continuity equation:

$$\frac{\partial \rho}{\partial t} = -\frac{\partial \vec{j}}{\partial x}. \quad (5)$$

We can easily generalize it for three dimensions:

$$\frac{\partial \rho}{\partial t} = -\nabla \cdot \vec{j}, \quad (6)$$

Where $\rho \equiv |\psi|^2$ is the probability density, and $\vec{j} \equiv \frac{i\hbar}{2m} (\psi \nabla \psi^* - \psi^* \nabla \psi)$ which is called *probability flux* or *quantum probability current*. In electrodynamics, the *continuity equation* represents the conservation of charge, which is not an independent assumption; rather, it is built into the laws of electrodynamics.

The continuity equation also provides a constraint in the values of ρ and \vec{j} , we cannot have any values of ρ and \vec{j} they have to respect the conservation of charge [8].

Similarly, we can interpret equation (4) as representing local conservation of probability as $|\psi|^2$, which is probability density [4].

By using $z - z^* = 2i \operatorname{Im}(z)$ where z is a complex number, and $\operatorname{Im}(z)$ represents the imaginary part of z , then the quantum probability current \vec{j} can be written as:

$$\vec{j} = -\frac{i\hbar}{2m} (\psi^* \nabla \psi - \psi \nabla \psi^*) = \frac{\hbar}{m} \operatorname{Im}(\psi^* \nabla \psi). \quad (7)$$

Next, we decompose the wave function ψ into polar form:

$$\psi = R e^{\frac{i}{\hbar} S}. \quad (8)$$

where R and S are real-valued functions representing, respectively, the amplitude and phase of the wave function. We can express the probability density in terms of the amplitude as $\rho = R^2$ and make the following substitution:

$$\psi^* \nabla \psi = R \nabla R + \frac{i}{\hbar} R^2 \nabla S. \quad (9)$$

The quantum probability current thus becomes:

$$\vec{j} = \frac{\hbar}{m} \text{Im}(R\nabla R + \frac{i}{\hbar} R^2 \nabla S) = \frac{\hbar}{m} \frac{R^2 \nabla S}{\hbar} = \frac{R^2 \nabla S}{m}, \quad (10)$$

which we can rewrite (using the relation $\rho = R^2$) as follows:

$$\vec{j} = \frac{\rho \nabla S}{m} = \rho v, \quad (11)$$

defining the velocity term as:

$$v \equiv \frac{\nabla S}{m}. \quad (12)$$

The implication of the quantum continuity equation with the realist interpretation of \vec{j} gives us the guiding equation (11) of Bohmian mechanics. However, Sakurai and Napolitano warn the readers on the literal interpretation of \vec{j} (as ρ times the velocity defined at every point in space) as a simultaneous measurement of position and velocity, which will violate the uncertainty principle [2].

5. Conclusion

We argued that quantum mechanics has a good and robust mathematical formalism and lacks a good interpretation of reality. We also presented a well-known problem in quantum mechanics: the measurement problem. And its possible solutions, in particular, we looked at the orthodox solution and why it does not give a satisfactory solution. We then explored another solution, the hidden variables, and how it solved the problem and presented the postulates of Bohmian mechanics. We then derived the quantum continuity equation and realistically interpreted the quantum probability current \vec{j} and showed that by interpreting \vec{j} as a real phenomenon, we arrive at the guiding equation in Bohmian mechanics.

Acknowledgments

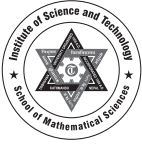
We would like to thank the anonymous referee(s) for their suggestions and comments.

References

- [1] Albert, D. Z. (1994). *Quantum Mechanics and Experience*. Harvard University Press.
- [2] Bohm, D. (1952). A suggested interpretation of the quantum theory in terms of "hidden" variables. I. *Physical Review*, **85**(2): 166–179.
- [3] Bohm, D. (1952). A suggested interpretation of the quantum theory in terms of "hidden" variables. II. *Physical Review*, **85**(2): 180–193.
- [4] Dirac, P. A. M. (1981). *The Principles of Quantum Mechanics* (27th ed). Oxford University Press.

- [5] Einstein, A., Podolsky, B., & Rosen, N. (1935). Can the quantum-mechanical description of physical reality be considered complete? *Physical Review*, **47(10)**: 777–780.
- [6] Griffiths, D. J. (2023). *Introduction to Electrodynamics*. Cambridge University Press.
- [7] Matarese, V. (2023). *The metaphysics of Bohmian mechanics: A Comprehensive Guide to the Different Interpretations of Bohmian Ontology* (Vol. 51). Walter de Gruyter GmbH & Co KG.
- [8] Ney, A., & Albert, D. Z. (2013). *The Wave Function: Essays on the Metaphysics of Quantum Mechanics*. Oxford University Press.
- [9] Norsen, T. (2017). *Foundations of Quantum Mechanics*. Springer.
- [10] Reiter, W. L., & Yngvason, J. (Eds.). (2013). *Erwin Schrödinger – 50 years after* (pp. 9–36). EMS Press.
- [11] Sakurai, J. J., & Napolitano, J. (2020). *Modern Quantum Mechanics*. Cambridge University Press.
- [12] Schrödinger, E. (2003). *Collected Papers on Wave Mechanics* (Vol. 302, p. 46). AMS Chelsea Publishing.
- [13] Von Neumann, J. (2018). *Mathematical Foundations of Quantum Mechanics: New edition* (Vol. 53). Princeton University Press.

□□



Mathematical Approach for Estimating the Effective Reproduction Number for COVID-19 in Nepal with Data-Driven SIR Model

Shiva Hari Subedi^{1*} & Gyan Bahadur Thapa²

¹ Department of Applied Sciences, Thapathali Campus, Institute of Engineering, Tribhuvan University, Nepal

² Department of Applied Science and Chemical Engineering, Pulchowk Campus, Institute of Engineering, Tribhuvan University, Nepal

Corresponding Author: *ssubedi@tcioe.edu.np

Abstract: The Effective Reproduction Number (R_t) is a critical parameter for understanding infectious disease dynamics and informing public health interventions. This study introduces a methodological framework for estimating R_t to analyze COVID-19 transmission dynamics in Nepal. The observational approach uses the data of the COVID-19 in Nepal within a Susceptible-Infected-Removed (SIR) model, excluding vital dynamics. The time-dependent transmission and recovery rates are calculated using the data in the model equations, and then these parameters, along with epidemic data, are fed into an Long Short Term Memory (LSTM) neural network, which learns temporal patterns from the data to improve prediction accuracy. The LSTM predicted parameters are applied into the formula to estimate R_t derived by the Next Generation Matrix method. The estimated values of R_t are validated against empirically observed data. Model performance is assessed using multiple metrics including mean absolute error (MAE), mean square error (MSE), root mean square error (RMSE) and coefficient of determination (r^2) to quantify the accuracy of predictions. This methodology enables quantitative assessment of epidemic trajectories and control measures, contributing to our understanding of COVID-19 dynamics in Nepal.

Keywords: COVID-19, SIR model, transmission dynamics, effective reproduction number, RNN-LSTM

1 Introduction

COVID-19, transmitted by the SARS-CoV-2 virus, rapidly became a pandemic with wide-ranging impacts, affecting health, economy, education systems, and social interactions internationally [15, 25]. National and international authorities showed efforts to control its spread by applying lockdowns, travel restrictions, mask-wearing, social distancing, large-scale testing, and the rapid development of vaccines while the researchers played a vital role by informing them with appropriate ideas for control strategies. The spread of COVID-19 in Nepal has been shaped by both global trends and local factors especially causing significant challenges during its second wave (spread of delta variant). The Susceptible-Infected-Removed (SIR) model with transmission rate (β) and recovery rate (ρ) provides a structured and analytical way to understand the spread of COVID-19, inform public health strategies, predict epidemic trajectories, estimate key parameters, and assess herd immunity. A data-driven approach makes the study more accurate, adaptable, and analytical by using real-time data to identify patterns and inform evidence-based decisions.

The effective reproduction number (R_t) is a fundamental concept in epidemiology, and is defined as the average number of secondary infections caused by a single infected individual at a particular time [5]. It is a key indicator in epidemiology to estimate the current transmission risk of a disease. From an epidemiological context, $R_t > 1$, $R_t < 1$, and $R_t = 1$ indicate a growing, declining and stable epidemic respectively [13]. The value of R_t may be influenced by immunity levels of individuals, virus variants, meteorological factors, and especially, by the interventions and control measures [10].

This study aims to perform a comparative analysis of the observed R_t values with those calculated using the predicted $\beta(t)$ and $\rho(t)$ in the Next Generation Matrix (NGM) formulation of the SIR model. The time-varying parameters $\beta(t)$ and $\rho(t)$ are estimated by feeding the data into the Recurrent Neural Network-Long Short Term Memory (RNN-LSTM) model, designed to capture temporal dependencies and learn patterns in the data over time. The outcomes of this analysis can contribute to infectious disease epidemiological studies in the context of Nepal. The rest of the paper includes a literature review, methodologies, the theoretical framework of the model, results with discussion, and some applications in Sections 2 to 6, respectively. Finally, Section 7 for conclusions summarizes the major findings of the paper, sharing some future directions.

2 Literature Review

The foundational SIR model introduced by Kermack et al. [14] established the groundwork for subsequent developments. Diekmann et al. [9] provided a comprehensive framework for defining and computing the basic reproduction number (R_0) in infectious disease models for heterogeneous populations, introducing the NGM approach. Since R_0 is more useful in theoretical models and can predict the nature of the outbreaks in the early stages but is less useful for tracking dynamical changes in real-world epidemics [8], many researchers [3, 12, 17] have emphasized the importance of the time-varying reproduction number for real-time monitoring of disease dynamics. Several epidemiological studies have focused on predicting R_t using compartmental modeling with universal differential equation approaches, statistical modeling techniques, and machine learning methods. Flaxman et al. [10] used a Bayesian framework to calculate R_t for COVID-19 in various countries. Mizumoto et al. [19] investigated the transmission potential of COVID-19 aboard the Diamond Princess cruise ship using mathematical modeling with time-series data. They found that the mean R_t reached up to 11 in the confined setting, but decreased significantly after quarantine measures were implemented. Arvanitis et al. [2] used a machine learning approach to predict R_t of COVID-19 in Greece and demonstrated a high accuracy in R_t prediction, which can support short-term policy and decision making. Cori et al. [6] developed a non-parametric approach for estimating R_t based on the time series of reported cases and the serial interval, utilizing an exponential growth model. Gostic et al. [11] evaluated methods for estimating the effective reproduction number (R_t) in near real-time and recommended the approach by Cori et al. They reported that accurate R_t estimation requires proper data preprocessing, effective delay handling, and precise specification of the generation interval. Ariel et al. [4] considered a single-outbreak SIR model and its corresponding estimation procedure for R_t using sensitivity analysis and statistical theory, demonstrating its application on synthetic data. They found that while the methods performed well in ideal conditions, problems were revealed through model fit diagnostics, highlighting the need for uncertainty estimation and residual analysis in SIR-type models. Cowling et al. [7] extended estimation methods for R_t during the H1N1 pandemic in Hong Kong, integrating reporting delays with continuous inflows. Their finding indicated that R_t declined from 1.4 – 1.5 at the beginning of the local epidemic to around 1.1 – 1.2 later, suggesting that changes were influenced by factors like school vacations or seasonality. Song et al. [24] proposed a method for estimating R_t using deep neural networks embedded in differential equations. Using data from Ontario's first wave of COVID-19 cases, they found that their deep learning approach performed better with fewer data sources. Nishiura et al. [20] analyzed time-dependent nature of R_t using renewal theory and concluded that the instantaneous reproduction number (R_t) changes abruptly over time, whereas the cohort reproduction number varies smoothly. Li et al. [16] reviewed different researches in infectious disease epidemiology to provide basic guidance into the selection and estimation methods for R_0 and R_t . They determined that the generation interval-based approach offers essential insights into the transmission dynamics of the diseases and supports the estimation of reproduction numbers. Within the scope of COVID-19 in Nepal, Pantha et al. [22] examined province-wise data from March 29, 2020, to September 27, 2020, analyzing key indicators such as epidemic patterns, growth rates, and reproduction numbers. They found that the maximum values of R_t range from 1.20 to 2.86 with the minimum value approximately 0.16. Pokhrel et al. [23] used data-driven SEIR model to analyze dynamics of COVID-19 in Nepal and estimated the median R_t during March 24 – June 01, 2020, to be 1.48 (with a minimum of 0.58 and a maximum of 3.71). Adhikari et al. [1] analyzed COVID-19 Delta variant data in Nepal to study its transmission nature and determined value of R_t up to 4.2 at the beginning of second wave (June 2021 to December 2021) and approximately 2.0 at the peak time of epidemic.

3 Methodologies

The methodologies employed in this study are both descriptive and predictive in nature, utilizing a computational modeling approach that combines mathematical modeling, data analysis, machine learning techniques, and statistical indicators. The main approaches applied to conduct the study are summarized in the Table 1.

Table 1: Methodologies Applied in the Study

SN	Components	Methods/Techniques	Remarks
1	Model	SIR model without vital dynamics	Assuming homogeneous mixing and constant population
2	Data Collection	Data retrieval from WHO, Our World in Data	Retrieving daily data of S, I, R, R_t in Nepal from 2020/5/8 to 2022/12/31
3	Data Preprocessing	Normalization, Nonlinear smoothing, Outliers removal	To reduce divergent scales, noise, outliers and overfitting
4	Prediction of β and ρ	RNN-LSTM Neural network	Input: $[S, I, R, \beta, \rho]$; Target: $[\beta, \rho]$
5	Calculation of R_t	Next generation matrix	To compute R_t
6	Stability Analysis	Jacobian eigenvalue analysis	To analyze stability at equilibrium points
7	Performance Metrics	MAE, MSE, RMSE, r^2	To evaluate the accuracy of the methods
8	Programming	MATLAB	To simulate and analyze the model

4 Theoretical Framework of SIR Model Dynamics

This section covers the theoretical concepts of the model, epidemic terminologies, the derivation of the effective reproduction number, and an analysis of stability.

4.1 Model Equations

The basic SIR model with constant population N (excluding new births and natural deaths) is described by the following transmission diagram (Fig. 1) and the system of differential equations (1)-(3). Here, $S = S(t)$, $I = I(t)$ and $R = R(t)$ denote the number of individuals in susceptible, infected and removed compartments, respectively, at any time t .



Figure 1: Flow diagram of the SIR model.

$$\frac{dS}{dt} = -\beta \frac{SI}{N} \tag{1}$$

$$\frac{dI}{dt} = \beta \frac{SI}{N} - \rho I \tag{2}$$

$$\frac{dR}{dt} = \rho I \tag{3}$$

System of ODEs for the SIR model

At initial stage, $S(0) = S_0$, $I(0) = I_0$, $R(0) = R_0$, satisfying $S_0 + I_0 + R_0 = N_0$ (the initial population). By summing and integrating the system of ODEs, we obtain $S(t) + I(t) + R(t) = C$ (a constant). Applying the initial conditions yields $S(t) + I(t) + R(t) = N_0 = N$, since N is assumed to be constant throughout the model.

4.2 Key Terminologies in the SIR Model

- i. **State Variables (S, I, R):** The state variables in the SIR model are susceptible individuals (S), who are at risk of becoming infected; infected individuals (I), who are currently infected with the disease and are infectious, and the removed (recovered+dead) individuals (R), who have either recovered or died from the disease.

- ii. **Transmission Rate (β)** : In the compartmental model β represents the product of contact rate and the probability of transmission per contact, and it is often referred to as the transmission rate.
- iii. **Recovery Rate (ρ)**: It is the rate at which infected individuals recover from the disease and transition into the R-compartment.
- iv. **Infection Rate ($\beta SI/N$)**: The infection rate $\beta SI/N$ in epidemic models represents the rate at which new infections are occurring in the population, specifically the rate at which susceptible individuals become infected.
- v. **Basic Reproduction Number (R_0)**: It represents the average number of secondary infections generated by a single infected individual in a fully susceptible population. R_0 is calculated at the early stage of an epidemic when the population is assumed to be entirely susceptible, and no interventions have been implemented.
- vi. **Effective Reproduction Number (R_t)**: It represents the average number of secondary infections caused by a single infected individual at time t during the course of the epidemic. R_t is calculated at any given time, so it reflects the current dynamics of the epidemic, considering factors such as population immunity (from previous infection or vaccination), public health interventions, and behavioral changes. It provides real-time overview into whether the disease is spreading ($R_t > 1$), stable ($R_t = 1$), or declining ($R_t < 1$).
- vii. **Infectious Period ($1/\rho$)**: The infectious Period ($1/\rho$) refers to the average duration an individual remains infectious and capable of transmitting the disease to others. After completing this period, the infected individuals enter the R compartment, either recovering or dying.
- viii. **Diseases Free Equilibrium (DFE)**: It is the state of the population in which there are no infectious individuals, and the disease cannot spread. It serves as a critical point in the analysis of epidemic models, particularly when evaluating the probability for an epidemic to occur or to be controlled.
- ix. **Endemic Equilibrium (EE)**: It is the stable state of a disease in a population where the disease stays at a constant level over time, without causing an outbreak or completely dying out.
- x. **Epidemic Threshold (ET)**: It is the condition under which a disease becomes endemic in the population, meaning it can persist at a constant level over time rather than dying out. Key factor analyzing endemic threshold is R_0 (for a non-immune and non-intervened population) or R_t (for an immune and intervened population).

4.3 Formulation of R_t using NGM

From the model equations (1)-(3), the ODE for the infected sub-population can be rearranged into two terms as:

$$\frac{dI}{dt} = \beta \frac{SI}{N} - \rho I = P - Q$$

where $P = \beta \frac{SI}{N}$ (new infection term) represents the inflow to infected compartment and $Q = \rho I$ (transition term) represents the outflow from the same compartment. P captures the transmission of infection and Q captures the progression of infection (in this case, recovery) whereas together they determine how the infection spreads through the population.

The Jacobian of P and Q with respect to I (say F and V respectively) can be derived as follows:

$$J[P(I)] = \left[\frac{\partial P}{\partial I} \right] = \left[\frac{\beta S}{N} \right] = F$$

$$J[Q(I)] = \left[\frac{\partial Q}{\partial I} \right] = [\rho] = V$$

The next generation matrix is

$$NGM = FV^{-1} = \left[\frac{\beta S}{N} \right] \left[\frac{1}{\rho} \right] = \left[\frac{\beta S}{N} \frac{1}{\rho} \right]$$

Since the NGM is 1×1 matrix, it has only one eigenvalue $\lambda = \frac{\beta S}{\rho N}$. The effective reproduction number R_t is the spectral radius (dominant eigenvalue) of NGM, so,

$$R_t = \frac{\beta S}{\rho N}$$

This gives the average number of secondary infections caused by a single infected individual in the remaining susceptible population at time t . When $t = 0$ (at the beginning of the epidemic), $S \cong N$ so that $R_0 \cong \frac{\beta}{\rho}$ which is the basic reproduction number.

4.4 Equilibrium Points and Stability Analysis

Equilibrium points of a system of ODEs for SIR model exist when the system is in steady state, *i.e.* when

$$\frac{dS}{dt} = 0, \quad \frac{dI}{dt} = 0, \quad \frac{dR}{dt} = 0$$

So in this state,

$$-\beta \frac{SI}{N} = 0, \quad \beta \frac{SI}{N} - \rho I = 0, \quad \rho I = 0$$

Disease Free Equilibrium (S^*, I^*, R^*) occurs when $I^* = 0$, so that $S^* + I^* + R^* = N$ gives $S^* + R^* = N$. Assuming the classical condition for the DFE, where the entire population remains susceptible in the absence of infection [9], we can set $R^* = 0$ to get $(S^*, I^*, R^*) = (N, 0, 0)$.

Endemic equilibrium (S^{**}, I^{**}, R^{**}) occurs when $I^{**} > 0$ and since $I^{**} \neq 0$, the second equation $\beta \frac{S^{**} I^{**}}{N} - \rho I^{**} = 0$ gives $\beta \frac{S^{**}}{N} = \rho$ or $S^{**} = \frac{\rho N}{\beta}$. Therefore, EE is $(S^{**}, I^{**}, R^{**}) = (\frac{\rho N}{\beta}, I_E, R_E)$, where I_E and R_E denote the number of infected and removed individuals respectively at the EE point.

The stability of the system of ODEs can be analyzed by determining the eigenvalues of their Jacobian matrix at the equilibrium points.

The Jacobian matrix for system of ODEs (1)-(3) is given by

$$J(S, I, R) = \begin{pmatrix} \frac{\partial}{\partial S}(\frac{dS}{dt}) & \frac{\partial}{\partial I}(\frac{dS}{dt}) & \frac{\partial}{\partial R}(\frac{dS}{dt}) \\ \frac{\partial}{\partial S}(\frac{dI}{dt}) & \frac{\partial}{\partial I}(\frac{dI}{dt}) & \frac{\partial}{\partial R}(\frac{dI}{dt}) \\ \frac{\partial}{\partial S}(\frac{dR}{dt}) & \frac{\partial}{\partial I}(\frac{dR}{dt}) & \frac{\partial}{\partial R}(\frac{dR}{dt}) \end{pmatrix} = \begin{pmatrix} -\frac{\beta I}{N} & -\frac{\beta S}{N} & 0 \\ \frac{\beta I}{N} & \frac{\beta S}{N} - \rho & 0 \\ 0 & \rho & 0 \end{pmatrix}$$

At DFE point $(S^*, I^*, R^*) = (N, 0, 0)$:

$$J(S^*, I^*, R^*) = \begin{pmatrix} 0 & -\beta & 0 \\ 0 & \beta - \rho & 0 \\ 0 & \rho & 0 \end{pmatrix} = \begin{pmatrix} 0 & -\beta & 0 \\ 0 & \beta - \rho & 0 \\ 0 & 0 & 0 \end{pmatrix}, \quad (\text{performing Row}_3 = \text{Row}_1 + \text{Row}_2 + \text{Row}_3)$$

Therefore, eigenvalues of $J(S^*, I^*, R^*)$ are $\lambda = 0, \beta - \rho, 0$. The zero eigenvalue does not provide necessary information about stability. The eigenvalue $\beta - \rho$ gives the progression rate of the infections, which determines whether the epidemic will grow, decay, or become stable near equilibrium.

- $\beta - \rho > 0 \implies \frac{\beta}{\rho} > 1 \implies R_0 > 1 \implies$ the epidemic is unstable, and the disease will spread exponentially.
- $\beta - \rho < 0 \implies \frac{\beta}{\rho} < 1 \implies R_0 < 1 \implies$ the disease is unstable and will eventually die out.
- $\beta - \rho = 0 \implies \frac{\beta}{\rho} = 1 \implies R_0 = 1 \implies$ the disease is in a stable endemic state.

At EE point $(S^{**}, I^{**}, R^{**}) = (S_E, I_E, R_E)$, where $S_E = \rho N / \beta$:

$$J(S^{**}, I^{**}, R^{**}) = \begin{pmatrix} -\frac{\beta I_E}{N} & -\frac{\beta S_E}{N} & 0 \\ \frac{\beta I_E}{N} & \frac{\beta S_E}{N} - \rho & 0 \\ 0 & \rho & 0 \end{pmatrix} = \begin{pmatrix} 0 & -\rho & 0 \\ \frac{\beta I_E}{N} & \frac{\beta S_E}{N} - \rho & 0 \\ 0 & \rho & 0 \end{pmatrix}, \quad (\text{performing Row}_1 = \text{Row}_1 + \text{Row}_2)$$

i.e.,

$$J(S^{**}, I^{**}, R^{**}) = \begin{pmatrix} 0 & 0 & 0 \\ \frac{\beta I_E}{N} & \frac{\beta S_E}{N} - \rho & 0 \\ 0 & \rho & 0 \end{pmatrix}, \quad (\text{performing Row}_1 = \text{Row}_1 + \text{Row}_3)$$

Therefore, eigenvalues of $J(S^{**}, I^{**}, R^{**})$ are $\lambda = 0, \beta S_E / N - \rho, 0$. The eigenvalue $\beta S_E / N - \rho$ determines whether the disease is growing, decaying, or becoming stable at endemic equilibrium.

- $\beta S_E / N - \rho > 0 \implies \frac{\beta S_E}{\rho N} > 1 \implies R_t > 1 \implies$ the epidemic is unstable, and the disease is spreading exponentially (epidemic growth).
- $\beta S_E / N - \rho < 0 \implies \frac{\beta S_E}{\rho N} < 1 \implies R_t < 1 \implies$ the disease is unstable but towards disease-free stable state and is coming to an end.
- $\beta S_E / N - \rho = 0 \implies \frac{\beta S_E}{\rho N} = 1 \implies R_t = 1 \implies$ the system is in a marginally stable endemic state, where the disease persists at a constant level.

5 Results and Discussion

This section presents and discusses the outcomes of the RNN-LSTM method and NGM formula to predict epidemic dynamic parameters (β , ρ) and R_t , by displaying comparative plots of observed and predicted values (Figure: 2 & 3) and by tabling the performance metrics of the procedures (Table: 2 & 3).

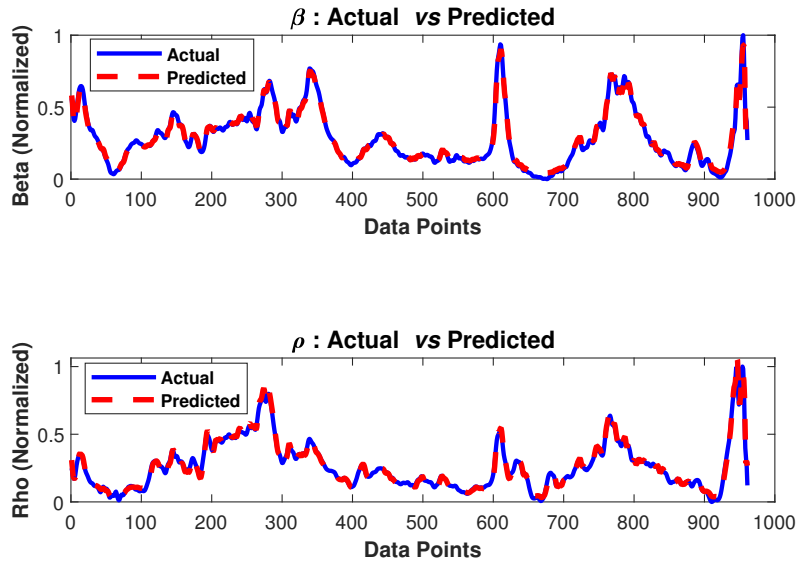


Figure 2: RNN-LSTM outcomes (for β and ρ)

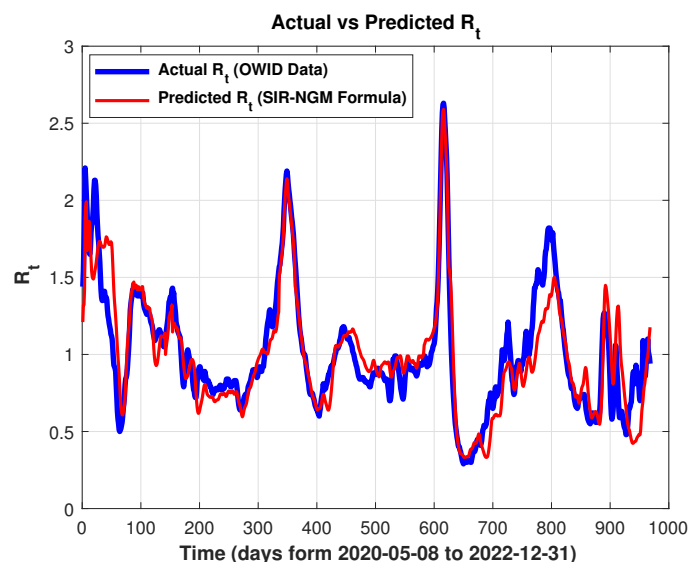


Figure 3: Actual (observed in OWID-data) and predicted (calculated by SIR-NGM-formula) R_t

Table 2: Performance metrics of RNN-LSTM predictions

Metric	Beta	Rho
MSE	0.00083214	0.00049888
RMSE	0.028847	0.022336
MAE	0.020822	0.017354
r^2	0.9774	0.97781

Table 3: Performance Metrics for Actual vs. Predicted R_t

Metric	Value
MAE	0.1249
MSE	0.0156
RMSE	0.1249
r^2	0.8984

In this study, the daily data for the compartments (S, I, R) and the time-varying reproduction number (R_t) were collected from reputable sources: the World Health Organization (WHO) [25] and Our World in Data (OWID) [21]. The preprocessed data for S, I, R and R_t were fed into a hybrid RNN-LSTM model to capture temporal dependencies in the time-series data. This model effectively predicted with greater accuracy, utilizing its ability to model complex, dynamic relationships over time. The NGM formulation was used to calculate R_t from the predicted values of β and ρ as a function of these time-varying parameters. This calculation helps for understanding the epidemic's potential to spread and evolve at each point in time.

The outcomes of the RNN-LSTM model are compared with the observed data values (Figure: 2), demonstrating that the model is an effective tool for predicting time-varying epidemic parameters. The performance metrics (Table: 2) further support the model's effectiveness. The observed and predicted values of β and ρ do not represent the actual epidemic values because the Rectified Linear Unit (ReLU) layer in the neural network normalizes the target values into the range of $[0, 1]$. However, this does not affect the calculation, as the ratio of beta and rho is sufficient for estimating R_t . Additionally, the graphs of β and ρ provide an information about their comparative impacts on the disease and expose the trends of the parameters over time. The similar trends of the parameters are due to the assumption that $S + I + R = N$ (constant) which implies $dS/dt = -dR/dt - dI/dt$ and due to the comparatively small number of infected individuals as well as their changes in the context of Nepal.

According to data from WHO [25], OWID [21], and information provided by the Ministry of Health and Population (MOHP) Nepal [18], the first wave of COVID-19 in Nepal began in May 2020 and lasted until early 2021, peaking in October. The second wave (Delta variant) occurred from April 2021 to October 2021. The third wave (Omicron variant) started in December 2021 and lasted until February 2022, peaking in January. OWID's growth rate-based estimation of R_t for Nepal closely matches the R_t calculated in this study using the SIR-NGM formula with LSTM-predicted parameters (Figure: 3). The fluctuation in the predicted R_t aligns with the COVID-19 waves

in Nepal. The low error and high r^2 values (Table: 3) further validate the findings. During the first wave, our study estimates R_t to range from 0.6 to 2.0, which is consistent with the study conducted by Pokhrel et al. [23]. During the peak of the second wave, our study has found that R_t exceeds 2, aligning with the findings of Adhikari et al. [1]. This suggests that the model, which utilizes the NGM formula and RNN-LSTM predictions, is effective in simulating the epidemic dynamics and estimating the reproduction number.

There are some limitations to this study. First, the study is based on the classical SIR model, assuming a constant and homogeneous population without considering age-based variations, which may not fully capture the actual epidemic dynamics of the whole country. Second, our main focus is on comparing R_t estimates to measure the effectiveness of the RNN-LSTM method within the classical SIR model, rather than analyzing the overall trend of R_t throughout the epidemic. So, the study does not consider the factors such as government interventions, vaccination coverage, population migration, hospital capacity, meteorological conditions which could affect the accuracy and applicability of our findings. The data collection process, methodology, and timing in Nepal significantly influence the outcomes of this study. Variations in data accuracy, inconsistencies in reporting, delays in updates, and differences in testing capacity can impact the estimation of R_t . Furthermore, under-reporting, changes in testing policies, and regional disparities in data availability may introduce biases, affecting the reliability of our findings.

6 Applications

The estimated R_t has diverse applications in epidemiological research including

- i. Performing real-time monitoring of disease spread.
- ii. Designing targeted intervention strategies.
- iii. Predicting the course of epidemics under different scenarios.
- iv. Assessing the impact of public health measures like vaccination.
- v. Estimating time varying transmission rate β if infectious period $1/\rho$ is known.
- vi. Evaluating variants of concern.
- vii. Assessing herd immunity threshold.

7 Conclusions

This study demonstrates the effectiveness of the hybrid RNN-LSTM model in predicting time-varying epidemic parameters (β and ρ) and estimating the effective reproduction number (R_t) using the SIR-NGM formulation. The predicted R_t closely aligns with observed values, capturing major fluctuations and reflecting COVID-19 waves in Nepal. The novel aspect of this study lies in the application of the neural network technique within a data-driven SIR model to achieve a refined parameter estimation approach in the context of Nepal. A higher accuracy in performance metrics provides strong scientific justification for the proposed approach, highlighting its effectiveness in capturing epidemic dynamics and improving predictive reliability. Since the model can be generalized for other countries, similar infectious diseases, different datasets, and varying conditions, it is adaptable to diverse epidemiological settings. Incorporating larger datasets and additional influencing factors further enhances the accuracy and robustness of predictions. The divergence between actual and predicted R_t in certain dates could be due to model limitations, data quality issues, and time lag in prediction. So, the limitations discussed in the previous section highlight the areas for improvement. In Nepal, data-driven studies face challenges like incomplete datasets, inconsistent collection, lack of standardization, manual entry errors, limited access, reporting delays, missing metadata, and resource constraints. Despite these constraints, the estimated R_t offers valuable insights for real-time disease monitoring, intervention strategies, and public health decision-making.

Future work will focus on refining the model by augmenting additional compartments with interventions, meteorological, and demographic factors which could provide a more comprehensive understanding of epidemic dynamics. This can be modified to perform qualitative analysis of R_t to predict the current state and future trajectory of an epidemic, helping to guide policy and public health decisions. To address the impact of poor data quality on the study, data preprocessing, cross-validation with multiple sources, uncertainty quantification, bias correction, sensitivity analysis, and transparent reporting can be employed.

References

- [1] Adhikari, K., Gautam, R., Pokharel, A., Dhimal, M., Uprety, K. N., & Vaidya, N. K. (2022). Insight into Delta variant dominated second wave of COVID-19 in Nepal. *Epidemics*, **41**: 100642.
- [2] Arvanitis, A., Furxhi, I., Tasioulis, T., & Karatzas, K. (2021). Prediction of the effective reproduction number of COVID-19 in Greece: a machine learning approach using Google mobility data. *J. Decis. Anal. Int. Comp.*, **1(1)**: 1–21.
- [3] Blumberg, S., & Lloyd-Smith, J. O. (2013). Inference of R_0 and transmission heterogeneity from the size distribution of stuttering chains. *PLoS Comput. Biol.*, **9(5)**: e1002993.
- [4] Cintrón-Arias, A., Castillo-Chávez, C., Bettencourt, L. M. A., Lloyd, A. L., & Banks, H. T. (2009). The estimation of the effective reproductive number from disease outbreak data. *Math. Biosci. Eng.*, **6(2)**: 261–282.
- [5] Contreras, S., Villavicencio, H. A., Medina-Ortiz, D., Saavedra, C. P., & Olivera-Nappa, A. (2020). Real-time estimation of R_t for supporting public-health policies against COVID-19. *Front. Public Health*, **8**: 556689.
- [6] Cori, A., Ferguson, N. M., Fraser, C., & Cauchemez, S. (2013). A new framework and software to estimate time-varying reproduction numbers during epidemics. *Am. J. Epidemiol.*, **178(9)**: 1505–1512.
- [7] Cowling, B. J., Lau, M. S. Y., Ho, L.-M., Chuang, S.-K., Tsang, T., Liu, S.-H., Leung, P.-Y., Lo, S.-V., & Lau, E. H. Y. (2010). The effective reproduction number of pandemic influenza: Prospective estimation. *Epidemiology*, **21(6)**: 842–846.
- [8] Delamater, P. L., Street, E. J., Leslie, T. F., Yang, Y. T., & Jacobsen, K. H. (2019). Complexity of the basic reproduction number (R_0). *Emerg. Infect. Dis.*, **25(1)**: 1–4.
- [9] Diekmann, O., Heesterbeek, J., and Metz, J. (1990). On the definition and the computation of the basic reproduction ratio R_0 in models for infectious diseases in heterogeneous populations. *J. Math. Biol.*, **28(4)**: 365–382.
- [10] Flaxman, S., Mishra, S., Gandy, A., Unwin, H.J.T., Mellan, T.A., Coupland, H., Whittaker, C., Zhu, H., Berah, T., Eaton, J.W., Monod, M., Imperial College COVID-19 Response Team, Ghani, A.C., Donnelly, C.A., Riley, S., Vollmer, M.A.C., Ferguson, L.C., & Bhatt, S. (2020). Estimating the effects of non-pharmaceutical interventions on COVID-19 in Europe. *Nature*, **584(7820)**: 257–261.
- [11] Gostic, K. M., McGough, L., Baskerville, E. B., Abbott, S., Joshi, K., Tedijanto, C., Kahn, R., Niehus, R., Hay, J. A., De Salazar, P. M., Hellewell, J., Meakin, S., Munday, J. D., Bosse, N. I., Sherratt, K., Thompson, R. N., White, L. F., Huisman, J. S., Scire, J., Bonhoeffer, S., Stadler, T., Wallinga, J., Funk, S., Lipsitch, M., & Cobey, S. (2020). Practical considerations for measuring the effective reproductive number, R_t . *PLOS Comput. Biol.*, **16(12)**: 1–21.
- [12] Heesterbeek, H., Anderson, R. M., Andreasen, V., Bansal, S., De Angelis, D., Dye, C., Eames, K. T. D., Edmunds, W. J., Frost, S. D. W., Funk, S., Hollingsworth, T. D., House, T., Isham, V., Klepac, P., Lessler, J., Lloyd-Smith, J. O., Metcalf, C. J. E., Mollison, D., Pellis, L., Pulliam, J. R. C., Roberts, M. G., Viboud, C., & Isaac Newton Institute IDD Collaboration. (2015). ‘Modeling infectious disease dynamics in the complex landscape of global health. *Science*, **347(6227)**: aaa4339.

- [13] Keeling, M. J. & Rohani, P. (2008). *Modeling infectious diseases in humans and animals*. Princeton University Press.
- [14] Kermack, W. O., McKendrick, A. G., & Walker, G. T. (1927). A contribution to the mathematical theory of epidemics. *Proc. R. Soc. Lond. Series A*, **115(772)**: 700–721.
- [15] Kumar, V., Alshazly, H., Idris, S. A., & Bourouis, S. (2021). Evaluating the impact of COVID-19 on society, environment, economy, and education. *Sustainability*, **13(24)**: 13642.
- [16] Li, K., Wang, J., Xie, J., Rui, J., Abudunaibi, B., Wei, H., Liu, H., Zhang, S., Li, Q., Niu, Y., & Chen, T. (2023). Advancements in defining and estimating the reproduction number in infectious disease epidemiology. *China CDC Wkly*, **5(37)**: 829–834.
- [17] Lipsitch, M., Cohen, T., Cooper, B., Robins, J., Ma, S., James, L., Gopalakrishna, G., Chew, S., Tan, C., Samore, M., Fisman, D., & Murray, M. (2003). Transmission dynamics and control of severe acute respiratory syndrome. *Science*, **300(5627)**: 1966–1970.
- [18] Ministry of Health and Population, Nepal (2020–2022). MOHP Nepal: COVID-19 Updates and Situation Reports. Available at: <https://www.moHP.gov.np>.
- [19] Mizumoto, K. & Chowell, G. (2020). Transmission potential of the novel coronavirus (COVID-19) onboard the diamond Princess Cruises Ship. *Infect. Dis. Model.*, **5**: 264–270.
- [20] Nishiura, H. & Chowell, G. (2009). The Effective Reproduction Number as a Prelude to Statistical Estimation of Time-Dependent Epidemic Trends: In *Mathematical and Statistical Estimation Approaches in Epidemiology*, 103–121. Springer Netherlands, Dordrecht.
- [21] Our World in Data. (2020–2022). COVID-19 Data Explorer. Available at: <https://docs.owid.io/projects/etl/api/covid/> Accessed: [2024-08-20].
- [22] Pantha, B., Acharya, S., Joshi, H. R., & Vaidya, N. K. (2021). Inter-provincial disparity of COVID-19 transmission and control in Nepal. *Sci. Rep.*, **11**: 13363.
- [23] Pokhrel, A. K., Joshi, Y. P., & Bhattarai, S. (2020). Epidemiological trend of COVID-19 in Nepal and the importance of social distancing to contain the virus. *Applied Sci. Tech. Ann.*, **1(1)**: 15–25.
- [24] Song, P. & Xiao, Y. (2022). Estimating time-varying reproduction number by deep learning techniques. *J. Appl. Anal. Comput.*, **12(3)**: 1–13.
- [25] World Health Organization. (2020–2022). Coronavirus disease (COVID-19) pandemic/WHO Coronavirus (COVID-19) Dashboard/WHO Nepal: COVID-19 Situation Reports. Available at: <https://www.who.int/nepal> Accessed: [2024-03-30].

□□

Instruction to Authors

Nepal Journal of Mathematical Sciences (NJMS)

1. Scope

Nepal Journal of Mathematical Sciences (NJMS) is the official peer-reviewed journal published by the School of Mathematical Sciences, Tribhuvan University. It is devoted to publishing original research papers as well as critical survey articles related to all branches of pure and applied mathematical sciences. The journal aims to reflect the latest developments in issues related to Applied Mathematics, Mathematical Modelling, Industrial Mathematics, Biomathematics, Pure and Applied Statistics, Applied Probability, Operations Research, Theoretical Computer Science, Information Technology, Data Science, Financial Mathematics, Actuarial Science, Mathematical Economics and many more disciplines. NJMS is published in English and it is open to authors around the world regardless of nationality. It is published two times a year. NJMS articles are freely available online and in print form.

2. Editorial Policy

NJMS welcomes high-quality original research papers and survey articles in all areas of Mathematical Sciences and real-life applications at all levels including new theories, techniques and applications to science, industry, and society. The authors should justify that the theoretical as well as computational results they claim really contribute to Mathematical Sciences or in real-life applications. A complete manuscript be no less than 5 pages and no more than 20 pages (11pt, including figures, tables, and references) as mentioned in the paper Template. However, this can be extended with the acceptance of the respective referees and the Editor-in-Chief. The submitted manuscript should meet the standard of the NJMS.

3. Manuscript Preparation

Manuscript must be prepared in Microsoft Word format (see Template) and LATEX (see template) in the prescribed format with a given page limit.

4. Title of the Paper

The title of the paper should be concise, and specific, not exceeding 15 words in length.

5. Authors Names and Institutional Affiliations

This should include the full names, institutional addresses, and email addresses of authors. The corresponding author should also be indicated.

6. Abstract and Keywords

Each article is to be preceded by an abstract up to a maximum of 250 words with 4-6 key pertinent words.

7. Introduction

The introduction briefly describes the problem, purpose, significance, and output of the research work, including the hypotheses being tested. The current state of the research field should be reviewed carefully and key publications should be cited.

8. Materials and Methods

It describes the research plan, the materials (or subjects), and the method used. It explains in detail the data, sample and population, and the variables used.

9. Results and Discussions

The results section should provide details of all of the experiments that are required to support the conclusions. Discussion can also be combined with results.

10. Figures and Tables

Figures and Tables are to be separately numbered, and titled in the text serially.

11. Conclusions and Acknowledgments

Not mandatory, but can be added to the manuscript.

12. References

•Journal Citation

[1] Faraji, H. & Nourouzi, K. (2017). Fixed and common fixed points for (ψ, ϕ) -weakly contractive mappings in b-metric spaces. *Sahand Communications in Mathematical Analysis*.7(1): 49-62.

•Doctoral Dissertation Citation

[1] Oliver, T. H. (2009). *The Ecology and Evolution of Ant-Aphid Interactions* (Doctoral dissertation Imperial College London).

•Research Book Citation

[1] Mursaleen, M. and Başar, F. (2020). *Topics in Modern Summability Theory*. BocaRaton : CRC Press.

13. Manuscript Submission

At the time of submission, authors are requested to include a list of 3-5 panelists of experts in the related research area. All information, submissions, and correspondence of the articles should be addressed to

Mailing Address: njmseditor@gmail.com

Nepal Journal of Mathematical Sciences (NJMS)

ISSN: 2738-9928 (Online), 2738-9812 (Print)

Volume 5, Number 1, February 2024

CONTENTS

SN	Article Titles and Authors	Page No.
1.	An Integral Involving Generalized Hypergeometric Function □ <i>Ganesh Bahadur Basnet, Narayan Prasad Pahari, Resham Prasad Paudel, Madhav Prasad Poudel & Mukesh Sharma</i> DOI: https://doi.org/10.3126/njmathsci.v5i1.76446	1-6
2.	Study of Common Fixed Point Theorems for Interpolative Contraction in Metric Space □ <i>Surendra Kumar Tiwari & Jayant Prakash Ganvir</i> DOI: https://doi.org/10.3126/njmathsci.v5i1.76442	7-14
3.	Security of E-health Image in Cloud Environment Using Hybridization of DNA Cryptography: Systematic Literature Review □ <i>Madhav Dhakal & Subarna Shakya</i> DOI: https://doi.org/10.3126/njmathsci.v5i1.76443	15-28
4.	A Short Note in Quantum Continuity Equation □ <i>Bishnu Hari Subedi & Tara Bahadur Rana</i> DOI: https://doi.org/10.3126/njmathsci.v5i1.76448	29-34
5.	Mathematical Approach for Estimating the Effective Reproductive Number for COVID-19 in Nepal with Data-Driven SIR Model □ <i>Shiva Hari Subedi & Gyan Bahadur Thapa</i> DOI: https://doi.org/10.3126/njmathsci.v5i1.76447	35-44

Mailing Address:

Nepal Journal of Mathematical Sciences

School of Mathematical Sciences

Tribhuvan University, Kirtipur, Kathmandu, Nepal

Phone: (00977) 01-6200207

Website: www.sms.tu.edu.np

Email: njmseditor@gmail.com

The Nepal Journal of Mathematical Sciences (NJMS) is now available on NepJOL

at <https://www.nepjol.info/index.php/njmathsci/index>